Ecological Indicators 148 (2023) 110143

Contents lists available at ScienceDirect

Ecological Indicators

journal homepage: www.elsevier.com/locate/ecolind

Original Articles

Kuznets and the cities: Urban level EKC evidence from Europe

Massimiliano Carlo Pietro Rizzati [a,*], Nicolò Florenzio [b], Gianni Guastella [c], Stefano Pareglio [c]

[a] Fondazione Eni Enrico Mattei, Corso Magenta, 63, 20123 Milano, MI, Italy
[b] Università Bocconi, GREEN (Centre for Research in Geography, Resources, Environment, Energy and Networks), Via Röntgen n. 1, 20136, Milano, MI, Italy
[c] Università Cattolica del Sacro Cuore, Dipartimento di Matematica e Fisica 'Niccolò Tartaglia', Via della Garzetta 48, 25123 Brescia, BS, Italy

ARTICLE INFO

Keywords:
Cities
Environment
Pollution
Environmental Kuznets Curve
Spatial Panel Econometrics

ABSTRACT

This paper empirically explores the extent to which European cities are on track to sustainable development by examining the environmental performance of a large sample of cities observed during the last two decades. The paper builds on the Environmental Kuznets Curve framework and leverages satellite data to build a set of environmental indicators as varied and as granular as possible. Evidence suggests that European cities are, on average, on track to sustainable development, meaning that the contribution of their economic growth to environmental degradation is already negative or close to becoming so. The paper also examines Transnational City Networks as accelerators of environmental transition. The results suggest that cities participating in such networks anticipate the transition with respect to their peers.

1. Introduction

Cities are hotspots of economic, social, and human development. People and firms choose to locate in dense urban areas to benefit from reduced commuting costs (Krugman, 1991), labour pooling opportunities (Overman and Puga, 2010), and knowledge transmission (Jacobs, 1969). Not surprisingly, in 2019, cities accounted for more than 80% of global GDP (WEF, 2022) and are projected to contribute to over 60% of global GDP growth between 2012 and 2030 (Floater et al., 2014). However, accelerated demand for housing, well-connected transport systems, infrastructure, and jobs may spur critical environmental degradation in multiple dimensions, especially air pollution, land use, biodiversity loss, and greenhouse gas (GHG) emissions. According to the United Nations Environmental Program report "Cities and Climate Change" (UNEP, n.d.), cities contribute to 75% of global carbon emissions (Dent et al., 2016), and it is estimated that they will account for over half of global energy-related emission growth between 2012 and 2030 (Floater et al., 2014). In addition, cities will add 1.2 million km^2 of new urban built-up areas around the globe in the next three decades (World Bank, 2022).

Cities and their policies are crucial to achieving the sustainability transition, but the empirical analysis of their environmental progress is still underdeveloped. The Environmental Kuznets Curve hypothesis (EKC), which predicts an inverse U-shaped relationship between environmental degradation and economic development, suggests that economies at advanced development stages naturally begin reducing their environmental footprint and even invest in environmental restoration. Despite the relevance of cities in the sustainability transition, few studies have examined cities and metropolitan areas as a unit of reference (Fujii et al., 2018; Wang et al., 2022) for the empirical estimation of the EKC relationship. In Europe, such studies have considered subnational units in a single country (Germani et al., 2020; Pontarollo and Serpieri, 2020) and, to the authors' knowledge, no research has focused on a multi-country set of cities. Overall, the existing literature provides an incomplete picture of how European cities, on the whole, are progressing with the multiple environmental aspects related to the sustainability transition. For this reason, it is crucial to expand the EKC analysis' scope beyond a single environmental degradation indicator and consider all the cities in Europe rather than a single country.

In light of the urgency of environmental action-taking at the city level, multiple Transnational City Networks (TCNs) have developed in the past few decades. These are intended to provide international platforms, allowing local governments to share best practices and generate political momentum around their environmental agenda. For instance, in relation to climate mitigation, member cities follow common protocols for monitoring emissions (Kona et al., 2021) and are encouraged to enforce more stringent environmental targets than non-members (Kona et al., 2018). If effective, the participation of cities in such networks is expected to change their environmental recovery pattern, arguably improving the sustainability of these cities (Labaeye and Sauer,

* Corresponding author.
E-mail address: massimiliano.rizzati@feem.it (M.C.P. Rizzati).

https://doi.org/10.1016/j.ecolind.2023.110143
Received 22 June 2022; Received in revised form 2 March 2023; Accepted 10 March 2023
1470-160X/© 2023 The Authors. Published by Elsevier Ltd. This is an open access article under the CC BY-NC-ND license (http://creativecommons.org/licenses/by-nc-nd/4.0/).

2013). Rashidi and Patt (2018) reported evidence that TCNs have effectively pushed global cities to take environmental action, but the extent to which these actions effectively improve the environmental performance of cities remains uncertain. TCNs are a relatively recent phenomenon, but a few have strong historical roots and are now being institutionalised (Acuto and Leffel, 2021). For that reason, it is important to understand whether a relationship exists between TCN participation and the environmental performance of cities.

This paper combines the EKC framework with the evidence of TCNs to empirically investigate the extent to which European cities effectively join the sustainability transition pathway by improving their environmental quality at certain stages of development and what the TCN's contribution is in this process. Europe represents an ideal setting for this study for multiple reasons. The first is the significant urban population exposure to air pollution (EEA, 2022). The second is a documented urban spatial expansion almost decoupled from population dynamics (Guastella et al., 2019). The third is the broad European representativeness in TCNs (Acuto and Leffel, 2021). The fourth is European cities' strong political mandate on environmental and climate action. Compared to Chinese or American counterparts, European cities have been given a central role in the low-carbon transition by their central governments in the framework of the Green Deals (UN-Habitat, 2020).

This work contributes to two different strands of literature. Firstly, it expands the EKC research stream by bringing novel evidence and testing the hypothesis using satellite imagery of environmental degradation in European cities. While the use of satellite imagery in the EKC framework is not new (Wang and Ye, 2017; Zheng and Kahn, 2017), these existing analyses are limited to Chinese cities. To the authors' knowledge, only one European study has used satellite imagery data to test the EKC (Altıntaş and Kassouri, 2020), but it looked at aggregate country-level indicators and missed both the spatial dimension and the granularity of the data. A few other studies have used lower administrative levels and spatial techniques, but these focused only on land use, neglecting the air pollution and emission-related aspects of environmental performance. Furthermore, they focused only on one country, namely Italy (Bimonte and Stabile, 2017) and Romania (Pontarollo and Serpieri, 2020). In both cases, the spatial unit of observation is the region, not the city.

Secondly, this paper contributes to the literature on TCNs, being the first study of its kind to measure the actual environmental benefits of participating in a network. The only comparable paper in the TCN literature is that by Hsu et al. (2020) who estimated that members of the EU Covenant of Mayors outperform non-members in their emission reduction targets. Other studies, such as Rashidi and Patt (Rashidi and Patt, 2018), used TCN information to explain policy action-taking without linking it to environmental performance directly. This study uses TCN information in a novel way, examining not only if TCN participation has a relationship with overall environmental degradation, but also the extent to which participation affects the recovery trajectory of European cities.

The paper has the following structure. Firstly, Section 2 expands on the reasons for the focus on several indicators of environmental degradation, the use of satellite imagery, and consideration of the TCN's role. Furthermore, the methodology is outlined, and the data is presented in Section 3. After showing the estimations and commenting on the results in Section 4, the results are discussed in Section 5.

2. Motivation

With a sound theoretical framework and a ready-to-test reduced-form equation, the EKC has been one of the most successful and debated topics in applied environmental economics. Grossman and Krueger (1995) first verified the predicted inverse U-shaped relationship between income and environmental degradation for sulphur dioxide (SO_2) concentration, suggesting that countries might be able to reduce pollution at a particular stage of development and decouple economic growth from environmental degradation. Empirical evidence supporting the EKC hypothesis has been subject to criticism for issues related to the GDP normality assumption and heteroscedasticity (Stern et al., 1996), omitted variable bias (Cole, 2003), and cointegration (Galeotti et al., 2009), but recent evidence from a *meta*-analysis (Sarkodie and Strezov, 2019) suggested that the hypothesis has survived the test of time.

2.1. Environmental degradation

One challenge in obtaining consistent cross-study estimates of the EKC hypothesis is the choice of the environmental degradation indicator. Greenhouse gas (GHG) emissions are probably the most investigated. Galeotti and Lanza (1999) found evidence of an inverted U-shaped curve for carbon dioxide (CO_2) using a quadratic panel regression on a dataset of 110 countries in the period 1960–1996. Their findings were later confirmed by several works, for example, Galeotti et al. (2006) for OECD countries and Wang and Ye, (2017) for 30 Chinese provinces. However, some studies concluded that the relationship between income and CO_2 emissions was monotonically increasing (Shafiei and Salim, 2014). Others discovered alternative cubic configurations, such as N-shaped curves (Sinha and Bhattacharya, 2017), while others discovered no EKC relationship at all (Acaravci and Ozturk, 2010; Zoundi, 2017). Sometimes, income has been substituted by alternative controls, such as urban form (Makido et al., 2012), urbanisation rate (Fang et al., 2021), and education (Maranzano et al., 2022).

Air pollutants are not climate warmers, but their effects on human health are severe and diverse, stemming from sub-clinical effects, ranging from inflammation to premature deaths. Selden and Song (1994) were the first to find evidence of an inverse U-curve for SO_2.[1] In a recent *meta*-analysis, Sarkodie and Strezov (2019) reviewed all the empirical papers that attempted to estimate the EKC and the relative turning point. Most papers, in their review, used atmospheric indicators to track pollution levels, and evidence supports the EKC hypothesis, although with substantial differences due to the varying period of study and econometric methods used in model estimation. More recently, the EKC has been tested for particulate matter in China (Zheng and Kahn, 2017; Ding et al., 2019).

Terrestrial and marine ecosystems have received relatively less attention in the EKC literature, and existing studies have focused primarily on land use. Liu and Guo (2015) estimated the EKC in Chinese provinces; Pontarollo and Serpieri (2020) for Romanian counties; Bimonte and Stabile (2017) for Italian NUTS-2 regions; Pontarollo and Muñoz (2020) for cantons in Ecuador. Alternative ecosystem-related indicators considered in the literature are the ecological footprint (Altıntaş and Kassouri, 2020), deforestation (Cuaresma et al., 2017), coal consumption (Hao et al., 2016), environmental crimes (Germani et al., 2020), e-waste (Boubellouta and Kusch-Brandt, 2020), and noise (Xu et al., 2020).

2.2. The spatial dimension

Some scholars have highlighted that many ecological metrics are not randomly distributed in space, and that ignoring the spatial dimension may lead to inaccurate results (Rupasingha et al., 2004). Before the diffusion of satellite imagery, the data were not sufficiently granular to allow spatial analysis of the EKC below the national state unit. Only recently have data on anthropogenic emissions become available at the metropolitan or city scale.Kang et al. (2019) and Wang et al. (2019) attempted to quantify them following international protocols for emission inventories. Other studies have relied on data scraping techniques to retrieve self-declared emissions at a municipal level (Hsu et al., 2020), and others have used concentration data for other pollutants instead of emissions (Ding et al., 2019). The sparser precision of these estimation

[1] See also Kaufmann et al. (1998).

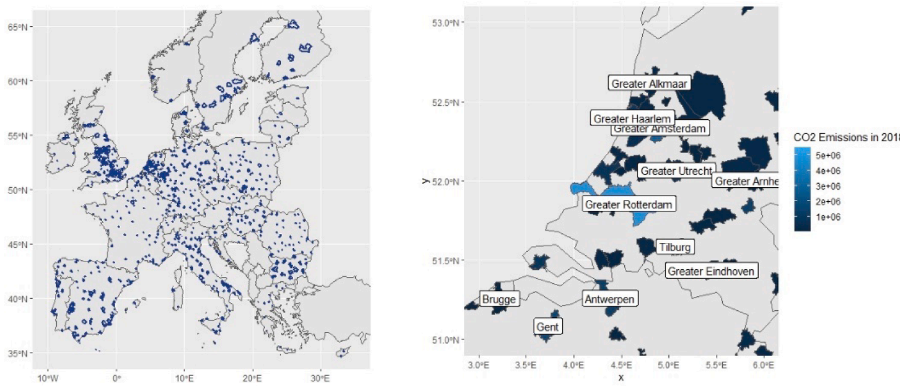

Fig. 1. Spatial structure of the sample. *On the left:* Fig. 1a, *administrative boundaries of the 922 cities in the sample. On the right:* Fig. 1b, *detail of the BENELUX area with total CO_2 emissions in 2018.*

Table 1
Description of the dependent variables.

Variable	Metric	Symbol	Description	Source
CO_2 Emissions[23]	tonne carbon/cell	CO_2	CO_2 emissions with a spatial resolution of approximately 1 × 1 km and a time resolution at the month level.	ODIAC (Oda et al., 2019)
O_3 Concentrations	μg/m^3	O_3	Ozone concentrations in AOT40 (Accumulated dose of ozone over a threshold of 40 ppb).	(EEA, 2018)
$PM_{2.5}$ Concentrations	μg/m^3	$PM_{2.5}$	Annual average concentrations global annual PM2.5 Grids from MODIS, MISR and SeaWiFS Aerosol Optical Depth (AOD) with GWR, v1 (1998 – 2016).	van Donkelaar et al. (2018)
Artificial area	Km^2	AA	Aggregated artificial surface codes in square kilometres.	Copernicus Corine Land Cover (CLC) dataset (European Union Copernicus Land Monitoring Service, 2000-2018)
SO_2	Mg/year	SO_2	Annual emission gridmaps at 0.1x0.1 degree resolution averaged per city.	Emissions Database for Global Atmospheric Research (EDGAR) (Crippa et al.,2022)

In this analysis, CO_2 emissions per capita was used as the dependent variable. For each city, the yearly total CO_2 emissions were divided by the urban population.

methods and the short spatio-temporal coverage of municipal bottom-up recordings (Gurney et al., 2019) pushes the researcher to find higher quality information.

Satellite imagery can provide spatially explicit and highly disaggregated observations, as well as independent data sources at various geographical scales. Direct satellite monitoring has the highest precision but has substantial limitations in detecting anthropogenic sources (Pan et al., 2021). Proxy satellite monitoring disaggregates national emission inventories using spatially distributed proxies like population density and night-time light data (Gurney et al., 2019; Oda et al., 2019).

Due to the granularity of its environmental data, proxy monitoring proves more reliable than self-reported data (Lauvaux et al., 2020);[2] enabling the use of spatial econometrics to estimate the EKC. For example, Wang and Ye (2017) interpolated the provincial CO_2 emissions in China with a combination of the areal interpolation method and night-time light data and tested the EKC hypothesis on a spatial dataframe. Ding et al. (2019) based their calculations on global satellite observation of $PM_{2.5}$ concentrations in the Beijing-Tianjin-Hebei area and found evidence of the existence of the EKC using multiple spatial econometric models.[3]

Another advantage provided by the combination of satellite imagery and spatial econometric methodology is the replicability of the analysis. Firstly, global emission inventories, such as the Open-source Data Inventory for Anthropogenic CO_2 (ODIAC) and the Emission Database for Global Atmospheric Research (EDGAR), have global coverage and provide comparable information for every location in the world, regardless of the level of development.[4] For example, Maddison (2006) used EDGAR data to test the EKC for 180 world countries (Wang et al., 2013). Despite its potential, to the authors' knowledge, no study has estimated the urban EKC in Europe with satellite imagery.

2.3. Cities and networks

Urbanisation is often linked to pollution (Wu et al., 2020) via multiple factors, including urban spatial expansion (Fragkias et al., 2013), traffic and congestion (Gately et al., 2015), and population growth (Ribeiro et al., 2019). In 2011, UN-Habitat released a debated report indicating that urban settlements were responsible for 40% to 70% of global GHG while occupying only 2% of land. In Europe, cities take up only 4% of total land (European Environment Agency, 2019) , but the 10 top emitter cities drive 33.4% of the total European carbon emissions Moran et al. (2022). If the EU is to deliver on the European Green Deal,[5] cities will have to be intimately involved in the climate mitigation effort.

On their part, European cities are demonstrating an increasing political will to be the vanguard of the efforts to achieve climate neutrality

[2] Satellite imagery is also comparable to bottom-up emission measurements at the city scale (Gurney et al., 2019).

[3] Other studies that used a spatial econometric methodology to test the EKC are Maddison (2006) and Wang et al. (2013) at the global level; Hao et al. (2016) and Kang et al. (2016) for China's regions; Pontarollo and Serpieri (2020) and Pontarollo and Munoz (2020) at the regional level for Romania and Ecuador.

[4] ODIAC was selected as the CO_2 emission data source for this work, as it provides better emission estimates and has a larger temporal resolution than EDGAR (Yang et al., 2020).

[5] According to the European Green Deal, the EU is to become climate neutral by 2050 and to reduce GHG emissions by 55% by 2030.

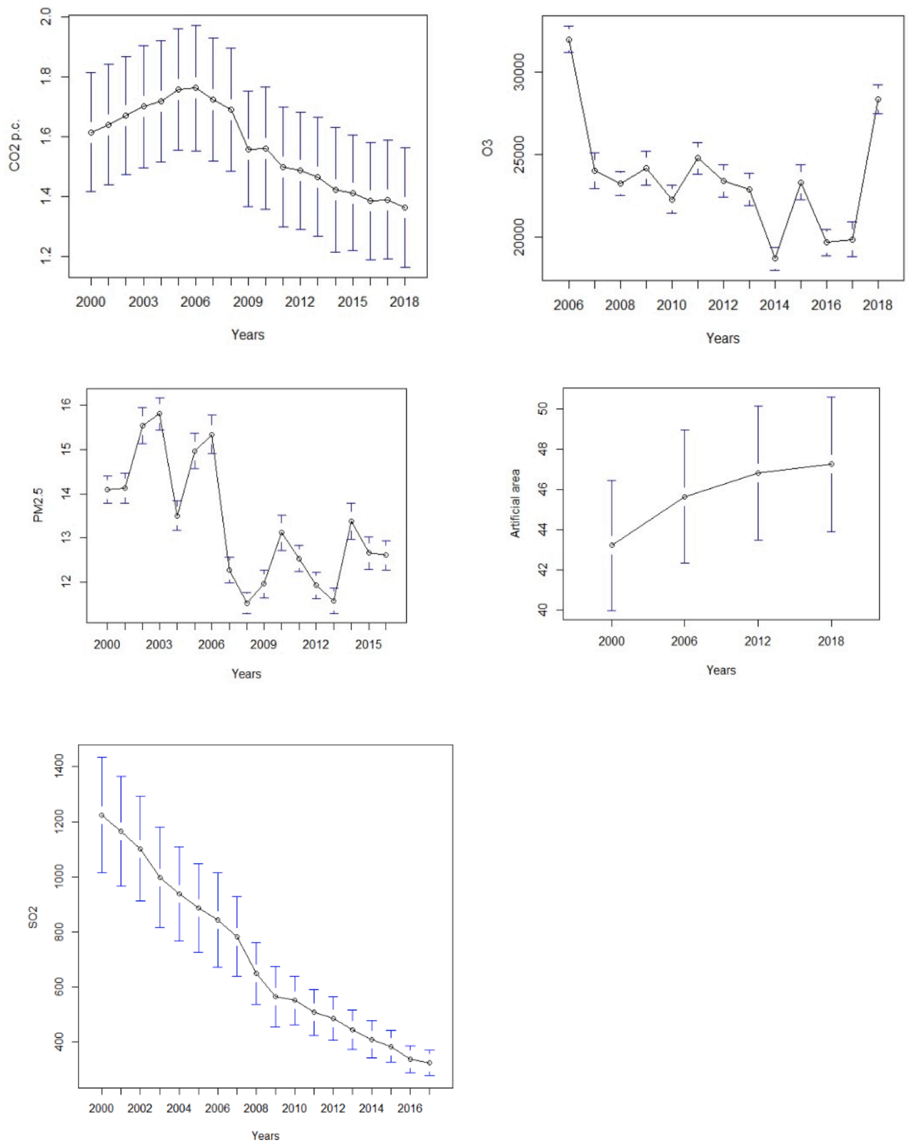

Fig. 2. Average trend of environmental indicators. Yearly averages for the five environmental indicators over the whole sample. CO_2 Emissions are in tonnes per capita. Standard deviation is in blue. (For interpretation of the references to colour in this figure legend, the reader is referred to the web version of this article.)

Table 2
Diagnostic tests: results for serial autocorrelation and spatial correlation.

Test	CO_2	O_3	$PM_{2.5}$	*Landuse*	SO_2
Breusch-Pagan Test	<2.2e-16	<2.2e-16	<2.2e-16	<2.2e-16	<2.2e-16
Pesaran Test	1.509e-07	<2.2e-16	3.775e-04	<2.2e-16	<2.2e-16
Breusch-Godfrey/ Wooldrdige	<2.2e-16	<2.2e-16	<2.2e-16	<2.2e-16	<2.2e-16
Baltagi, Song and Koh (marginal)	<2.2e-16	<2.2e-16	<2.2e-16	<2.2e-16	<2.2e-16
Baltagi, Song and Koh (conditional)	<2.2e-16	<2.2e-16	<2.2e-16	<2.2e-16	<2.2e-16
Moran I statistic $t = 1$ (p-value)	0.062 (0.000)	0.360 (0.000)	0.121 (0.000)	0.063 (0.000)	0.006 (0.312)
Moran I statistic $t = T$ (p-value)	0.070 (0.000)	0.433 (0.000)	0.280 (0.000)	0.038 (0.001)	0.006 (0.305)

Table 3
Estimation of the benchmark model. Estimation results for CO_2 emissions, O_3 and $PM_{2.5}$ concentrations, artificial land use (AA) and SO_2 emissions. Standard Errors in parenthesis. The model for $PM_{2.5}$ is fitted with GMM estimation.

	CO_2	O_3	$PM_{2.5}$	*AA*	SO_2
log*GDP*	1.631^{***}	-9.621^{**}	2.853^{***}	-3.116^{***}	-9.590^{***}
	(1.842)	(3.516)	(0.613)	(0.534)	(1.937)
log*GDP*^{2}	-0.058^{***}	0.896^{**}	-0.272^{***}	0.326^{***}	0.860^{***}
	(0.008)	(0.326)	(0.060)	(0.052)	(0.191)
log*GDP*^{3}	–	-0.028^{**}	0.008^{***}	-0.011^{***}	-0.024^{***}
		(0.010)	(0.001)	(0.001)	(0.006)
log*D*	-0.310^{***}	−0.003	0.058*	0.131^{***}	0.111^{**}
	(0.005)	(0.007)	(0.012)	(0.013)	(0.037)
log*T*	5.321^{***}	31.725^{***}	-9.978^{***}	4.010^{***}	-11.814^{***}
	(0.790)	(0.960)	(0.744)	(0.827)	(0.037)
CN	0.050^{***}	−0.024	0.027***	0.016	-0.083^{***}
	(0.013)	(0.015)	(0.003)	(0.003)	(0.010)
Time dummy	included				
ρ(spatial error parameter)	0.495^{***}	0.532^{***}	0.523^{***}	0.408^{***}	0.225^{***}
	(0.011)	(0.013)	(0.011)	(0.028)	(0.015)
Observations	17,518	11,986	15,674	3688	16,596
R^2	0.329	0.532	0.939	0.994	0.944

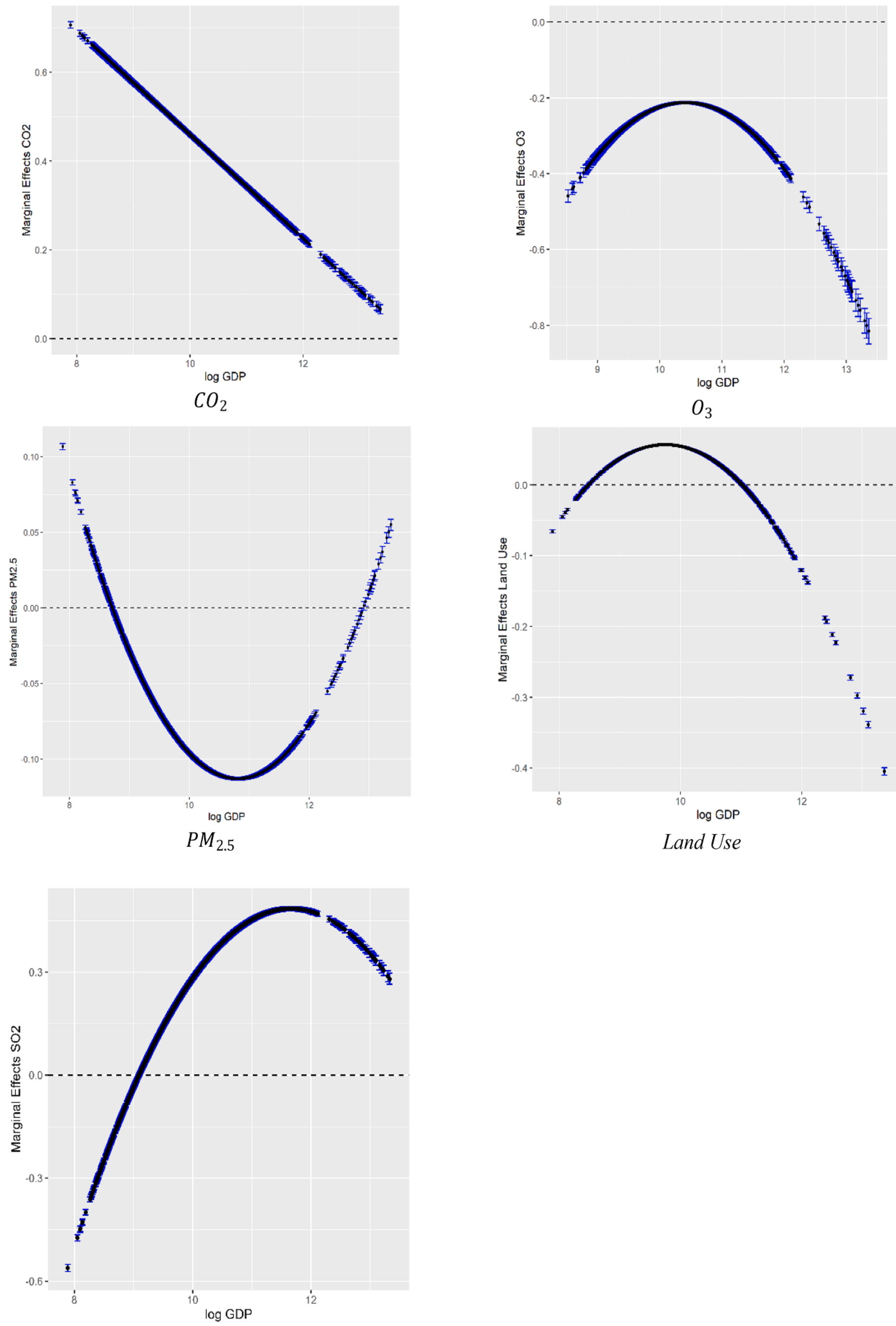

Fig. 3. Marginal effects – aggregate. Marginal effects of the selected environmental variables plotted against log(GDP).

with the rise of TCNs. These are membership-based alliances between local governments that provide a platform for implementing common policies and developing joint initiatives.[6] For example, the European members of the Covenant of Mayors signed an overall commitment to reduce emissions by 27% by 2020 (Kona et al., 2018), well above the minimum requested EU target of 20%. In addition, 64% of Eurocities members have already committed to becoming climate neutral by 2050. In 2016, the C40 Cities Climate Leadership Group (C40), the Global Covenant of Mayors for Climate & Energy, and the International Council for Local Environmental Initiatives (ICLEI) joined forces with the World Resources Institute (WRI) to develop the Global Protocol for Community-Scale Greenhouse Gas Emissions Inventories.

As momentum for TCNs' involvement in global mitigation efforts is growing, it is crucial to evaluate whether their participation effectively translates into better environmental performance. So far, the TCN literature has not produced a quantitative assessment on this specific point.[7] To the authors' knowledge, the only paper that evaluates cities' GHG emissions mitigation performance in the context of some transnational climate initiative is Hsu et al (2020), which calculated that 60% of more than 1,000 EU Covenant of Mayors' cities are on track to achieve their 2020 emission reduction targets.

[6] According to Acuto and Leffel (2021), globally TCNs number more than 200 and most of them (29%) are centred on environmental concerns. Nonetheless, the membership of networks shows a "Euro-centric bias".

[7] Most of the literature is focused on knowledge transfers and experimentation like Nguyen et al. (2020).

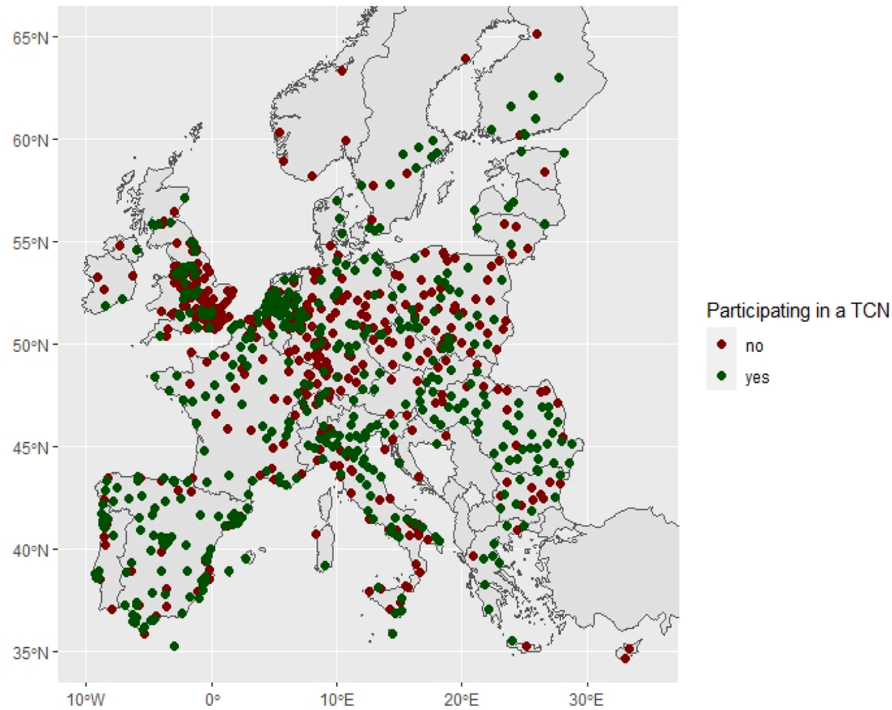

Fig. 4. Localisation of member and non-member cities. Member cities are in green (4 7 7), while non-member cities are in red (4 4 4). (For interpretation of the references to colour in this figure legend, the reader is referred to the web version of this article.)

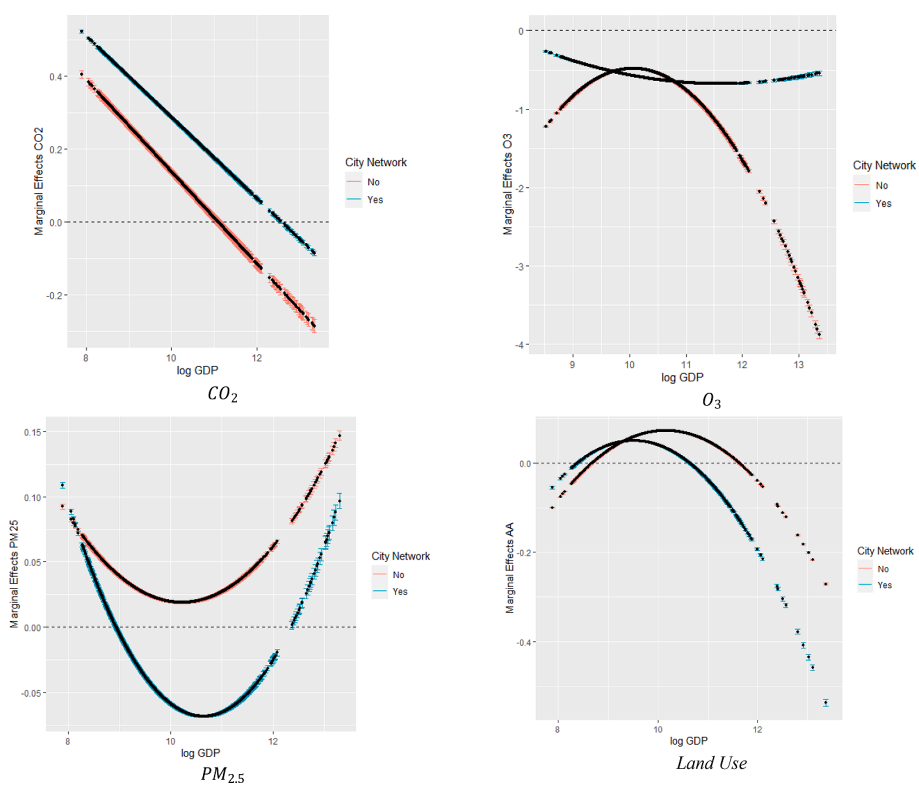

Fig. 5. Marginal effects of the selected environmental variables plotted against in GDP, after the sample split.

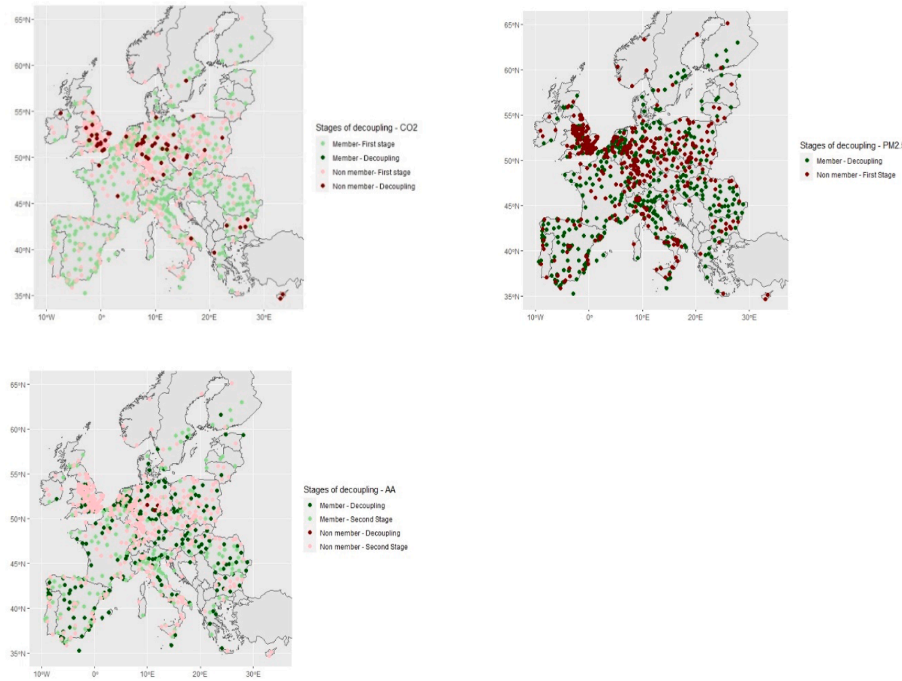

Fig. 6. Spatial distribution of decoupling cities.

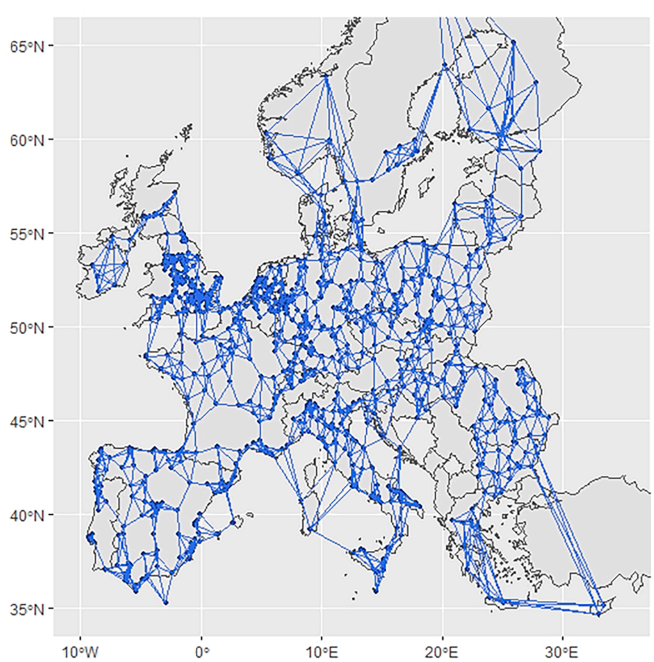

Fig. A1. Spatial weight matrix, selecting the 10 nearest neighbours each city.

3. Methodological approach and data

3.1. Methodology

Considering the different environmental degradation indicators, the EKC curve shape can be inferred by testing the signs of the coefficients of GDP per capita (Liu and Guo, 2015). Including a squared term and a cubic term of the latter allows the functional form and shape of the curve to be checked.

The EKC curve parameters are first estimated with standard panel data models (pooled OLS, random effects, and fixed effects). In the context of EKC estimation, this provides more comprehensive information and weakens the impact of multicollinearity, which could be present in time-series data (Ding et al., 2019). Moreover, since this study's data presents a micro-panel structure ($N > T$) the use of methods such as Autoregressive Distributed Lags (ARDL) is not recommended, and, overall, the issue of stationarity is mitigated by the inclusion of time effects (Baltagi, 2021).[8] As data from more years will become available in future, the analysis should also be reconsidered in the light of the effects of possible time distortions, for instance, with techniques such as panel cointegration (Cho et al., 2014) and non-stationary spatial panel data (Beenstock and Felsenstein, 2019).

The chosen EKC specification follows equation (1):

$$E_{i,t} = \propto + \beta_1 GDPpc_{i,t} + \beta_2 \left(GDPpc_{i,t}\right)^2 + \beta_3 \left(GDPpc_{i,t}\right)^3 + \gamma X_{i,t} + \delta N_{i,t} + \tau_t + \varepsilon_{i,t} \tag{1}$$

Here, $E_{i,t}$ is the environmental indicator observed in city i at year t. $GDPpc_{i,t}$ is the per-capita GDP, including its quadratic and cubic terms to capture potential non-linear relationships. X is a matrix of time-varying control variables, including population density and the average temperature; N is a dynamic dummy that is equal to 1 in the years when the city is part of a city network and 0 otherwise; τ is the time-specific effect, and ε the error term.

To account for the potential spatial dependence among the city-level environmental targets (Ding et al., 2019; Kang et al., 2016), a global Moran's I test and two Lagrange Multiplier diagnostics for spatial panel data were performed (Baltagi et al., 2007). The first LM diagnostic is a joint statistic that simultaneously tests for spatial error correlations and

[8] All of the series of indicators and time-varying variables were tested for non-stationarity with an IPS test with different combinations of lags, trends, and demean (Im et al., 2003), the Harris and Tsivalis test (Harris and Tzavalis, 1999) and the Pesaran test in the presence of cross-section dependence (Pesaran, 2007). The only variable series with unambiguous evidence of non-stationarity was population density, which becomes stationary in the first differences. As a robustness test, the estimation of Table 3 was carried out again with population density as a first difference, finding no qualitative change in the EKC shape parameters for all indicators.

Table A1
Top five cities for each indicator in the initial and final year of the sample, as well as the top five cities ranked for overall reduction in the indicator.

Indicator		2000 City	Country	Value	2018 City	Country	Value	2000–2018 City	Country	% reduction	City Network
CO_2	Tonne per capita	M. Konin	PL	62.8	M. Konin	PL	74.4	Westminster	UK	72.7%	N
		M. Rybnik	PL	23.1	M. Rybnik	PL	25.6	Camden	UK	72.4%	N
		Greater Middelburg	NL	23.0	Greater Middelburg	NL	19.3	City of London	UK	71.9%	Y
		Warrington	UK	20.8	Heilbronn	DE	16.3	Tower Hamlets	UK	70.2%	N
		Heilbronn	DE	20.0	M. Opole	PL	15.9	Islington	UK	69.3%	N
$PM_{2.5}$	µg/m3	Radom	PL	28.5	Padova	IT	31.7	Lugo	ES	61,55%	Y
		Tomaszów Mazowieck	PL	28.4	Venezia	IT	30.5	Santiago de Compostela	ES	59,82%	Y
		Piotrków Trybunalski	PL	28.1	Treviso	IT	30.1	Pontevedra	ES	57,89%	Y
		Sosnowiec	PL	28.1	Vicenza	IT	29.9	Ourense	ES	51,60%	N
		Krakow	PL	27.9	Krakow	PL	28.5	Cuenca	ES	50,22%	Y
O_3	µg/m3	Cremona	IT	64228.4	Chania	EL	67518.5	Avilés	ES	85,57%	Y
		L'Aquila	IT	63806.6	Lecco	IT	65829.8	Coruña, A	ES	80,41%	Y
		Massa	IT	63723.5	Como	IT	64986.1	Gijón	ES	69,96%	Y
		Piacenza	IT	62460.6	Busto Arsizio	IT	63397.2	Lugo	ES	69,24%	Y
		Saronno	IT	62158.9	Saronno	IT	63344.1	Oviedo	ES	67,70%	N
AA	Km^2	City of Paris	FR	700.9	City of Paris	FR	704.3	Ferrol	ES	27,58%	N
		Berlin	DE	574.0	Berlin	DE	562.9	Wigan	UK	26,82%	N
		Hamburg	DE	407.1	Hamburg	DE	401.2	Most	CZ	22,06%	N
		Roma	IT	365.2	Roma	IT	395.8	Görlitz	DE	15,68%	N
		Budapest	HU	330.9	Budapest	HU	348.5	Dessau-Roßlau	DE	15,29%	N
SO_2	Mg/year	Drobeta-Turnu Sever	RO	48696.7	Aviles	ES	8416.5	Tatabánya	HU	99,75%	N
		Craiova	RO	32809.9	Plock	PL	8132.0	Drobeta-Turnu Sever	RO	99,68%	N
		Konin	PL	32398.4	Linea de la Concepcion	ES	6667.8	Cannock Chase	UK	99,65%	N
		Linea de la Concepcion	ES	24289.6	Most	CZ	5712.7	Pecs	HU	99,44%	Y
		A Coruna	ES	21724.3	Duisburg	DE	4400.6	Serres	EL	98,79%	Y

random individual effects. The second is a marginal statistic that tests the existence of spatial error correlations, assuming the presence of random individual effects. The selected benchmark was the Spatial Error Model (SEM), which was estimated with pooling, fixed effects, and random effects methods. With a spatial error structure, the EKC-SEM becomes:

$$E_{i,t} = \propto + \beta_1 GDPpc_{i,t} + \beta_2 \left(GDPpc_{i,t}\right)^2 + \beta_3 \left(GDPpc_{i,t}\right)^3 + \gamma X_{i,t} + \delta N_{i,t} + \tau_t + u_i \tag{2}$$

$$u_i = \lambda W u_{i,t} + \varepsilon_{i,t}$$

Where the error u_i includes a spatial component modelled through the spatial error term $\lambda W u_{i,t}$, with λ being the autoregressive factor and W the spatial weight matrix. As the cities in the sample are, in the majority of cases, not contiguous, W was built by selecting a number of the nearest neighbours by distance.

Alternative spatial panel econometrics specifications, such as a spatial autoregressive model (SAR) or Spatial Durbin Model (SDM), are usually preferred to the SEM because they allow decomposing the marginal effect in a direct and an indirect – spatial spillover – effect. In contrast, the advantage of SEM over SAR and SDM is the more straightforward interpretation of coefficients and inference (Bivand et al., 2021). This advantage becomes determinant in the model choice when the model specification is non-linear and includes polynomial terms (or interaction terms), as in the EKC case, because the SEM marginal effects do not depend on the spatial parameters.

3.2. Data

This study adopted the definition of "city" from the GISCO Eurostat: "A city is a local administrative unit (LAU) where the majority of the population lives in an urban centre of at least 50 000 inhabitants".[9] The cities' shapefiles were recovered from GISCO Eurostat.[10] To avoid distortions and missing matches in the spatial weight matrix, outlier cities in the Azores, Canary Islands, and French overseas were excluded. This resulted in 922 cities from 20 countries, representing a collection of relevant urban centres that included wide and densely populated metropolitan areas and relatively smaller towns (Fig. 1a). It must be noted that some of the cities are located in the same administrative areas (NUTS-3).

Table 1 presents the selected environmental indicators. The indicators' grids are intersected with each urban administrative boundary and aggregated at the year level as spatial sums (emission, land cover) or averages (concentrations). In this way, a spatially distributed panel dataset was created (Fig. 1b). By observing the dataset, the best and the worst performers among the sample in terms of absolute values and reduction achievements can be extrapolated.[11] Notably, these rankings show some evidence of spatial dependence. For example, most of the top five cities with the highest concentrations of fine particulate matter ($PM_{2.5}$) and ozone (O_3) in 2018 are located in the Po Valley (Italy). On the contrary, the cities with the best performance in the reduction of the former are all located in Galicia (Spain) (Table A1).

Fig. 2 shows the evolution of the sample averages over time for the five environmental indicators. Overall, there has been a substantial reduction in environmental degradation from 2000 to 2018, in particular following the great financial crisis (2006–2008). On average, CO_2 per capita emissions have decreased by 18.4% in the sample period and

[9] See Eurostat (n.d.). "What is a city? Spatial units". Link: https://ec.europa.eu/eurostat/web/cities/spatial-units.
[10] © EuroGeographics for the administrative boundaries.
[11] For reference, see Table A1 in the Appendix.

Table A2
Description and sources of the independent and control variables.

Variable	Metric	Symbol	Description	Source
Income per capita	USD	GDP	Provincial Gross Domestic Product per capita in Purchasing Power Standard (PPS) in 2000–2018	(OECD, 2018)
Population density	Inhabitants/ km^2	PD	Population counts divided by the city area in square kilometres	Eurostat
Average temperature	°C	T	Annual average of the ERA5-Land temperature weighted for the city area in Celsius degrees	Muñoz Sabater (2019)
City Network	0–1	*CN*	Dummy variable. 0 = not in a city network; 1 = in a city network	Elaboration on considered city networks data (ICLEI – Local Governments for Sustainability, C40, Global Covenant of Mayors for Climate and Energy, 100 Resilient Cities)
Committment to a city network	Number of years	*CCN*	Commitment to a city network and numbers of years since joining one.	Elaboration on considered city networks data (ICLEI – Local Governments for Sustainability, C40, Global Covenant of Mayors for Climate and Energy, 100 Resilient Cities)
Mountain zone category		*MZC*	Category for mountain area type (0–6)	Kapos (2000)
Average Elevation	meters	*E*	Average elevation in the city area in meters over the sea	Eurostat, GISCO
Distances from borders	kilometers	*B*	Distance in Km from the closest other country border	Eurostat, GISCO
Distances from sea	kilometers	*S*	Distance in Km from the closest sea shore	Eurostat, GISCO

have been steadily declining since 2006 (-29.3%). O_3 concentrations shrunk by 41.7% from 2006 to 2014 and, notwithstanding their rebound in 2018, they are still 11.3% below their starting level. $PM_{2.5}$ concentrations showed some volatility over the years but altogether fell by 10.4% over the whole period. SO_2 emissions have constantly decreased since 2000 and registered the most significant downfall among the indicators (-73%). On the contrary, the artificial area surged by 9.4%.[12]

[12] These trends are in line with observations by EEA (2021). Discrepancies in these estimates may be due to the use of different satellite data sources and to the different spatial nature of the sample.

The sampled cities are diverse. Some are megacities placed in an industrial area, and some are small rural towns. Different demographic and geographical factors are considered to account for differences in size, population, and location. Controls included both time-varying and time-constant effects, presented in Table A2.[13] The study also considered the hypothesis that a city may participate in one or more TCNs dedicated to sustainable growth and climate change mitigation. Participation in these climate initiatives may be a symptom of environmental awareness and omitting this information may bias the estimates.[14]

4. Results

After running the set of non-spatial linear regressions,[15] the first evidence of cross-sectional dependence was collected with the Pesaran test (Table 2). In addition, the Breusch-Godfrey/Wooldridge test for panel models showed the presence of serial correlation. This issue was explored further by testing each variable for spatial correlation, using the Global Moran's I and the Lagrangian Multiplier tests from Baltagi et al. (2007). All the tests confirmed the presence of spatial correlation in the model (except for Moran's I for SO_2), providing a case for the use of spatial econometric techniques. Consequently, the EKC was estimated with an SEM.[16] In order to dispel any doubts about the chosen model, a specification that included both spatial lags and spatial errors was run and revealed that spatial errors were always more statistically significant than lags.[17] Then, the in-sample income turning points were bootstrapped. Finally, the results are discussed below.

4.1. Estimation results

Table 3 presents the results for the benchmark model. Following the related literature, the model variables are taken in logs. Time effects results are omitted to save space but are available in Table A12 of the Appendix. The spatial matrix *W* was built by considering the ten nearest neighbours. Although the structure of a spatial weight matrix could be less relevant to the estimation results than having a well-specified model (LeSage and Pace, 2014), the number of selected neighbours might affect them due to the large distances possible in the sample. A robustness exercise was conducted with varying neighbours' numbers to check that the signs of the coefficients were not affected.[18]

The estimation results confirm two main findings: the existence of spatial dependence[19] and the variety of EKC shapes. CO_2 emissions display the usual inverted U-shape, in line with Bölük and Mert (2014) and Kasman and Duman (2015) but in contrast with Acaravci and Ozturk (2010) and Altıntaş and Kassouri (2020). With regards to other geographical areas, Aldy (2005) finds the same inverted-U relation for U.S. states. An N-shaped relationship was found for $PM_{2.5}$; in contrast to Zheng and Kahn (2017) and Ding et al. (2019), who found an inverse

[13] Most of these controls are constant in time, so they do not appear in the benchmark fixed-effects model. However, they can still be observed in the nonspatial estimations. For the descriptive statistics of control variables, see Table A3 in the Appendix.

[14] Additional details of the selected city networks are included in Table A4 in the Appendix.

[15] See the estimation results from Table A5 to Table A9 in the Appendix.

[16] Estimations were performed on R through the packages *plm* (Croissant and Millo, 2008) for panel models and *splm* (Millo and Piras, 2012) for spatial panel models and the related statistics.

[17] This approach was proposed by Bivand et al. (2021) and the results can be found in the Appendix in Table A10.

[18] The spatial weight matrix W was constructed with the functions included in the R package *spdep* (Bivand et al., 2015).Visualisation of the spatial weight matrix can be found in Figure A1 of the Appendix. As a robustness check, *W* was also considered with K=5, K= 20, K=50. Results are listed in Table A11 of the Appendix.

[19] ρ has a significant and positive value in each specification.

Table A3
Summary statistics of all the variables considered in the study.

Statistics		Mean	St. Dev.	Min	1st qrtl.	3rd qrtl.	Max
Environmental degradation							
CO_2 emissions	Tonne per cell	1.57	3.11	0.08	0.63	1.44	74.37
$PM_{2.5}$ Concentrations	μg/m^3	13.340	5.36	1.02	9.54	15.78	45.44
O_3 Concentrations	μg/m^3	23,580.08	14,726.21	0.00	10,956.02	34,193.10	85880
Artificial areas (AA)	Km^2	45.74	51.32	1.26	19.72	53.45	704.29
SO_2 emissions	Mg/year	700.13	2088.487	2.04	74.74	487.42	48696.76
Controls							
Income per capita	USD	34305.34	28388.48	2167	22648	40002	638193
Population density	Inhabitants/km^2	2039.219	2174.81	22.23	782.69	2508.73	32868.77
Average temperature	°C	11.35	2.89	−1.67	9.52	13.04	20.99
Mountain zone category	1-7	0.54	1.35	0	0	0.08	6.33
Average elevation	M	174.50	194.40	−3.77	42.01	239.36	1298.61
Distance from closest border	Km	146.30	121.67	48.02	219.75	0.71	1283.07
Distance from closest sea	km	134	151.30	0.01	6.57	238.72	627.60
City network	0-1	0.52	0.50	0	0	1	1
Commitment to a city network	years	5.97	7	0	0	11	30

Table A4
Detail on the city networks considered; (1) source: City networks' websites, Wikipedia; (2) authors' calculation of the sample considered.

Name	Year of foundation[1]	Participants[2]
ICLEI – Local Governments for Sustainability	1990	83
C40	2005	16
Global Covenant of Mayors for Climate and Energy	2016	471
100 Resilient Cities	2013	11

U-shaped relationship between particulate matter and GDP in Chinese cities. For the remaining environmental indicators, there was an inverse N-shaped function. To the authors' knowledge, this paper is the first to find evidence of an EKC for ozone. With regard to SO_2, the only paper focused on Europe found an inverted U-shaped relationship (Rafaj et al., 2014)for 13 EU countries. Finally, the results on land use are in contrast to those of Bimonte and Stabile (2017), who rejected the EKC hypothesis for land consumption in Italian regions, and Pontarollo and Serpieri (2020), who found an inverted U-shape for 42 Romanian counties.

With regard to the control variables, the study estimates a significant and negative contribution of population density to CO_2 emissions, while the contribution to O_3 is statistically non-significant. Population density also shows significant and positive coefficients for $PM_{2.5}$, SO_2 and artificial area (AA). These results can be interpreted in light of recent data on emissions by source in Europe, in which road transport is the second most important contributor to CO_2, while residential and commercial activities are the main sources of $PM_{2.5}$ (Tiseo, 2022; EEA, 2022). Ozone precursors are mainly produced by agriculture and the residential sector, while energy supply is the biggest producer of SO_2 (EEA, 2022) . Thus, assuming that population density is positively correlated with the level of urban agglomeration, low CO_2 emissions can be expected in densely populated cities due to limited car usage. At the same time, densely populated areas are characterised by a high concentration of residential and commercial areas, leading to high levels of $PM_{2.5}$ and SO_2. Population density is also strictly linked to high shares of built-up areas in city centres. Finally, temperatures have a negative effect on $PM_{2.5}$ and SO_2, while they contribute to the increase in CO_2 emissions and O_3 and AA.

Finally, the relationships between environmental indicators and TCN participation are largely heterogeneous. Participating in a city network seems to be beneficial for the reduction of O_3 concentrations and SO_2 emissions. However, participation appears to be associated with higher CO_2 emissions, $PM_{2.5}$ concentrations, and AA. As a result, the role of city networks in the mitigation of environmental degradation is ambiguous. For this reason, it is explored in depth in Section 4.3.

4.2. Turning points

Turning points have been calculated in virtually every work on the EKC, but consensus on their entity has never been reached (Sarkodie and Strezov, 2019). Narrowing the focus to Europe, the estimated turning points for CO_2 emissions move in a wide range from 3,630 USD to 83,973.75 USD (Shahbaz and Sinha, 2019). For land use, the range is smaller, from 993 USD to 3,451 USD (Pontarollo and Serpieri, 2020). Rafaj et al. (2014) found the inflection point of their curve at around 13,000 USD for SO_2. Estimates of the turning point for $PM_{2.5}$ concentrations are not available for Europe, but Ding et al. (2019) located it between 80,508 and 106,903 yuan (from circa 11,000 USD to 14,000 USD) in Chinese NUTS-3 regions, in line with Zheng and Kahn (2017) who calculated the turning point at around 100,000 yuan. Finally, to the authors' knowledge, estimates for the turning point of O_3 concentrations are absent from the literature.

The turning point is the income level at which the marginal effect, supposed to be initially positive and decreasing, equals zero and later becomes negative. It is computed using the coefficient point estimates. While computationally straightforward, the approach does not allow any inference of the turning point. The confidence interval for marginal effects estimated in Section 4.1 was computed via bootstrap on sub-samples. In detail, the model was re-estimated 1,000 times using a random sub-sample of 600 units[20] and the marginal effect and confidence intervals at each level of GDP in the sample were computed. Fig. 3 presents the marginal effects plotted against the actual series of log(GDP) for all the selected indicators.

- The marginal effect of CO_2 is linearly decreasing, as expected, but the value of log (GDP) at which the effect becomes zero, and later negative, is out-of-sample. Although the inverse U-shape is correctly predicted by the model, a more accurate inference suggests that the EKC hypothesis is not verified in EU cities. In contrast, evidence indicates that emissions continue to grow as GDP increases, although at a decreasing pace.
- The $PM_{2.5}$ results return more EKC-consistent evidence. The marginal effect is positive and decreasing up to an approximate income level of 6,600 USD,[21] above which it turns negative. Notably, the

[20] The spatial weight matrix used in every run changes accordingly.
[21] Notably, this threshold for European cities is lower than those found by Zheng and Kahn (2017) and Ding et al. (2019) for Chinese cities.

Table A5
Panel estimation, full model for CO_2.

	Pooled	FE	RE
log_G	9.502*	−4.086	−4.700*
	(5.188)	(2.865)	(2.677)
log_G_2	−0.741	0.485*	0.554**
	(0.498)	(0.284)	(0.264)
log_G_3	0.020	−0.018*	−0.020**
	(0.016)	(0.009)	(0.009)
log_D	−0.334***	−1.040***	−0.833***
	(0.021)	(0.033)	(0.033)
log_Temp	−5.497**	−8.099***	−7.505***
	(2.203)	(0.805)	(0.786)
Avg_MNT	−0.035**		−0.048**
	(0.014)		(0.023)
Avg_elevation	−0.001***		−0.001***
	(0.000)		(0.000)
D_Bord_m	−0.000		−0.000
	(0.000)		(0.000)
D_Sea_m	0.000**		0.000
	(0.000)		(0.000)
N	0.001	0.021**	0.022**
	(0.040)	(0.010)	(0.010)
time2001	−0.023***	−0.009***	−0.011***
	(0.005)	(0.003)	(0.003)
time2002	0.009	0.046***	0.040***
	(0.007)	(0.007)	(0.007)
time2003	0.006	0.056***	0.048***
	(0.008)	(0.008)	(0.008)
time2004	−0.010	0.056***	0.046***
	(0.010)	(0.009)	(0.009)
time2005	0.020*	0.099***	0.086***
	(0.012)	(0.011)	(0.010)
time2006	−0.018	0.090***	0.071***
	(0.014)	(0.012)	(0.012)
time2007	−0.065***	0.061***	0.039***
	(0.017)	(0.014)	(0.014)
time2008	−0.121***	0.015	−0.009
	(0.019)	(0.016)	(0.015)
time2009	−0.195***	−0.062***	−0.086***
	(0.020)	(0.015)	(0.015)
time2010	−0.279***	−0.163***	−0.183***
	(0.024)	(0.016)	(0.016)
time2011	−0.308***	−0.172***	−0.196***
	(0.026)	(0.017)	(0.017)
time2012	−0.335***	−0.200***	−0.224***
	(0.027)	(0.018)	(0.018)
time2013	−0.380***	−0.240***	−0.265***
	(0.029)	(0.019)	(0.019)
time2014	−0.426***	−0.269***	−0.298***
	(0.032)	(0.020)	(0.020)
time2015	−0.430***	−0.268***	−0.298***
	(0.033)	(0.021)	(0.021)
time2016	−0.469***	−0.294***	−0.327***
	(0.036)	(0.023)	(0.023)
time2017	−0.482***	−0.296***	−0.332***
	(0.038)	(0.025)	(0.025)
time2018	−0.514***	−0.315***	−0.354***
	(0.041)	(0.026)	(0.026)
Constant	−6.805		60.294***
	(20.027)		(9.978)
Observations	17,518	17,518	17,518
R^2	0.278	0.559	0.528
Adjusted R^2	0.277	0.534	0.528
	***Significant at the 1 percent level.		

Notes: ***Significant at the 1 percent level.
**Significant at the 5 percent level.
*Significant at the 10 percent level.

Table A6
Panel estimation, full model for O_3.

	Pooled	FE	RE
log_G	9.502*	−4.086	−4.700*
	(5.188)	(2.865)	(2.677)
log_G_2	−0.741	0.485*	0.554**
	(0.498)	(0.284)	(0.264)
log_G_3	0.020	−0.018*	−0.020**
	(0.016)	(0.009)	(0.009)
log_D	−0.334***	−1.040***	−0.833***
	(0.021)	(0.033)	(0.033)
log_Temp	−5.497**	−8.099***	−7.505***
	(2.203)	(0.805)	(0.786)
Avg_MNT	−0.035**		−0.048**
	(0.014)		(0.023)
Avg_elevation	−0.001***		−0.001***
	(0.000)		(0.000)
D_Bord_m	−0.000		−0.000
	(0.000)		(0.000)
D_Sea_m	0.000**		0.000
	(0.000)		(0.000)
N	0.001	0.021**	0.022**
	(0.040)	(0.010)	(0.010)
time2001	−0.023***	−0.009***	−0.011***
	(0.005)	(0.003)	(0.003)
time2002	0.009	0.046***	0.040***
	(0.007)	(0.007)	(0.007)
time2003	0.006	0.056***	0.048***
	(0.008)	(0.008)	(0.008)
time2004	−0.010	0.056***	0.046***
	(0.010)	(0.009)	(0.009)
time2005	0.020*	0.099***	0.086***
	(0.012)	(0.011)	(0.010)
time2006	−0.018	0.090***	0.071***
	(0.014)	(0.012)	(0.012)
time2007	−0.065***	0.061***	0.039***
	(0.017)	(0.014)	(0.014)
time2008	−0.121***	0.015	−0.009
	(0.019)	(0.016)	(0.015)
time2009	−0.195***	−0.062***	−0.086***
	(0.020)	(0.015)	(0.015)
time2010	−0.279***	−0.163***	−0.183***
	(0.024)	(0.016)	(0.016)
time2011	−0.308***	−0.172***	−0.196***
	(0.026)	(0.017)	(0.017)
time2012	−0.335***	−0.200***	−0.224***
	(0.027)	(0.018)	(0.018)
time2013	−0.380***	−0.240***	−0.265***
	(0.029)	(0.019)	(0.019)
time2014	−0.426***	−0.269***	−0.298***
	(0.032)	(0.020)	(0.020)
time2015	−0.430***	−0.268***	−0.298***
	(0.033)	(0.021)	(0.021)
time2016	−0.469***	−0.294***	−0.327***
	(0.036)	(0.023)	(0.023)
time2017	−0.482***	−0.296***	−0.332***
	(0.038)	(0.025)	(0.025)
time2018	−0.514***	−0.315***	−0.354***
	(0.041)	(0.026)	(0.026)
Constant	−6.805		60.294***
	(20.027)		(9.978)
Observations	17,518	17,518	17,518
R^2	0.278	0.559	0.528
Adjusted R^2	0.277	0.534	0.528

Notes: ***Significant at the 1 percent level.
**Significant at the 5 percent level.
*Significant at the 10 percent level.

marginal effect becomes positive again after the threshold of 442,000 USD, suggesting there are a few outlier cities in the sample with very high income and also very high concentration levels.

- The O_3 marginal effect is negative at every GDP level, indicating that ozone concentration contracts as income rises in a non-monotonic fashion, showing a complete decoupling with economic development. The evidence clearly suggests that there is no support of the EKC hypothesis but, on the other hand, it also shows that there is no environmental issue with O_3 concentration being related to economic development.
- The SO_2 emissions results do not confirm the EKC hypothesis. On the one hand, the estimated marginal effect is initially lower than zero and later becomes positive after the approximate income threshold

Table A7
Panel estimation, full model for.$PM_{2.5}$.

	Pooled	FE	RE
log_G	2.494	2.379***	2.606***
	(1.670)	(0.689)	(0.607)
log_G_2	−0.258	−0.224***	−0.245***
	(0.158)	(0.068)	(0.059)
log_G_3	0.009*	0.007***	0.007***
	(0.005)	(0.002)	(0.002)
log_D	0.104***	0.016	0.082***
	(0.010)	(0.013)	(0.009)
log_Temp	−2.464**	−11.145***	−7.677***
	(1.219)	(0.801)	(0.793)
Avg_MNT	0.022***		0.014**
	(0.007)		(0.007)
Avg_elevation	−0.001***		−0.001***
	(0.000)		(0.000)
D_Bord_m	−0.001***		−0.001***
	(0.000)		(0.000)
D_Sea_m	0.001***		0.001***
	(0.000)		(0.000)
N	−0.075***	0.037***	0.034***
	(0.016)	(0.005)	(0.005)
time2001	−0.005	−0.020***	−0.014***
	(0.006)	(0.005)	(0.005)
time2002	0.083***	0.082***	0.082***
	(0.005)	(0.005)	(0.005)
time2003	0.115***	0.112***	0.112***
	(0.006)	(0.006)	(0.006)
time2004	−0.049***	−0.063***	−0.059***
	(0.007)	(0.006)	(0.006)
time2005	0.046***	0.030***	0.035***
	(0.008)	(0.006)	(0.007)
time2006	0.065***	0.067***	0.065***
	(0.010)	(0.009)	(0.009)
time2007	−0.123***	−0.117***	−0.121***
	(0.008)	(0.007)	(0.007)
time2008	−0.165***	−0.178***	−0.178***
	(0.009)	(0.008)	(0.007)
time2009	−0.151***	−0.174***	−0.175***
	(0.010)	(0.008)	(0.008)
time2010	−0.086***	−0.150***	−0.136***
	(0.014)	(0.011)	(0.011)
time2011	−0.070***	−0.098***	−0.100***
	(0.011)	(0.008)	(0.007)
time2012	−0.128***	−0.174***	−0.170***
	(0.012)	(0.009)	(0.009)
time2013	−0.157***	−0.213***	−0.207***
	(0.013)	(0.010)	(0.009)
time2014	−0.022	−0.045***	−0.052***
	(0.015)	(0.012)	(0.012)
time2015	−0.072***	−0.104***	−0.109***
	(0.014)	(0.012)	(0.011)
time2016	−0.061***	−0.099***	−0.102***
	(0.014)	(0.011)	(0.009)
time2017	0.010	−0.025*	−0.029**
	(0.016)	(0.013)	(0.011)
time2018	0.050***	0.027**	0.018
	(0.017)	(0.013)	(0.012)
Constant	8.049		36.513***
	(8.682)		(4.829)
Observations	17,518	17,518	17,518
R^2	0.526	0.389	0.396
Adjusted R^2	0.525	0.354	0.395

Notes: ***Significant at the 1 percent level.
**Significant at the 5 percent level.
*Significant at the 10 percent level.

of 8,000 USD. This, however, must be considered at the light of the decrease in European trends (Rafaj et al., 2014) and the low values found in this work.

- Finally, the land use results provide almost full support for the EKC hypothesis. This is defined as almost full because the AA's marginal effect is initially negative, which is inconsistent with the hypothesis. However, after an approximate income value of 4,000 USD, the marginal effect becomes positive, indicating that the artificial urban area increases with income and does so at increasing rates, which is consistent with the existing empirical evidence about the urban sprawl and inefficient land use phenomena operating in small cities (Guastella et al., 2017). The marginal effect decreases and becomes negative above the 60,000 USD income threshold. Cities above the threshold stop expanding the urbanised area and invest in urban reconversion projects, for instance, re-naturalising abandoned areas or investing in green urban infrastructures.

Table A8
Panel estimation, full model for Land use.

	Pooled	FE	RE
log_G	−24.596***	−4.046***	−4.590***
	(6.361)	(0.946)	(0.878)
log_G_2	2.462***	0.420***	0.468***
	(0.628)	(0.094)	(0.087)
log_G_3	−0.081***	−0.014***	−0.016***
	(0.021)	(0.003)	(0.003)
log_D	−0.067***	0.146***	0.077***
	(0.024)	(0.028)	(0.020)
log_Temp	−24.582***	4.258***	0.246
	(2.480)	(0.633)	(0.628)
Avg_MNT	−0.030		−0.007
	(0.021)		(0.023)
Avg_elevation	−0.001***		−0.001***
	(0.000)		(0.000)
D_Bord_m	0.001***		0.001***
	(0.000)		(0.000)
D_Sea_m	0.000**		0.001***
	(0.000)		(0.000)
N	0.369***	0.021***	0.023***
	(0.043)	(0.005)	(0.005)
time2006	0.001	0.058***	0.057***
	(0.014)	(0.005)	(0.005)
time2012	−0.172***	0.084***	0.074***
	(0.029)	(0.007)	(0.007)
time2018	−0.187***	0.065***	0.066***
	(0.043)	(0.010)	(0.010)
Constant	223.519***		16.210***
	(24.908)		(4.636)
Observations	3,688	3,688	3,688
R^2	0.237	0.420	0.337
Adjusted R^2	0.234	0.224	0.335

Notes:
***Significant at the 1 percent level.
**Significant at the 5 percent level.
*Significant at the 10 percent level.

4.3. The role of city networks

To explore the contribution of TCNs, the data were split into two sub-samples: cities that are members of at least one TCN and cities that are not. The spatial distribution of sample cities by the group to which they belong is displayed in Fig. 4. Interestingly, there are no signs of geographical concentration of member cities, while non-members appear to be particularly present in the United Kingdom, Germany, and Eastern Europe (mainly in the Czech Republic and Poland). In relative terms, Norway and Ireland are also predominantly represented by non-members.

An SEM benchmark regression was run for each of the two groups of cities. The resulting marginal effects are shown in Fig. 5. The latter does not include SO_2, as income loses statistical significance.

Overall, the two sub-samples exhibit similar behaviours. For example, both member and non-member cities display decreasing marginal effects of income on CO_2 emissions, with non-member cities reaching their turning point earlier (respectively at 60,000 versus 270,000 USD). Viewed from another angle, the evidence shows that non-member cities have, other things being equal, lower emission growth and that urban economic development in Europe has been coupled to carbon use and emissions. This interpretation is line with Wang et al.

Table A9
Panel estimation, full model for SO_2.

	Pooled	FE	RE
log_G	13.104***	−9.936***	−8.098***
	(3.430)	(1.991)	(1.967)
log_G_2	−1.441***	0.890***	0.719***
	(3.43)	(0.196)	(0.194)
log_G_3	−1.441***	−0.025***	−0.020**
	(0.327)	(0.006)	(0.006)
log_D	0.594***	0.099**	0.304***
	(0.009)	(0.038)	(0.027)
log_Temp	3.112**	−12.024***	−6.559***
	(1.031)	(2.188)	(1.941)
Avg_MNT	−0.096***	–	−0.078*
	(0.009)	–	(0.039)
Avg_elevation	−0.001***	–	−0.001**
	(0.000)	–	(0.000)
D_Bord_m	−0.000	–	−0.000
	(0.000)	–	(0.000)
D_Sea_m	0.001***	–	0.001***
	(0.000)	–	(0.000)
N	0.758**	−0.091***	−0.094***
	(0.025)	(0.010)	(0.010)
time2001	−0.008	−0.070***	−0.057***
	(0.056)	(0.016)	(0.0168)
time2002	−0.075	−0.144***	−0.138***
	(0.56)	(0.016)	(0.016)
time2003	−0.241***	−0.332***	−0.324***
	(0.056)	(0.016)	(0.016)
time2004	−0.260***	−0.405***	−0.388***
	(0.056)	(0.017)	(0.017)
time2005	−0.309***	−0.482***	−0.461***
	(0.057)	(0.018)	(0.017)
time2006	−0.366***	−0.571***	−0.554***
	(0.057)	(0.018)	(0.018)
time2007	−0.424***	−0.668***	−0.649***
	(0.057)	(0.019)	(0.019)
time2008	−0.485***	−0.767***	−0.738***
	(0.057)	(0.020)	(0.020)
time2009	−0.656***	−0.897***	−0.872***
	(0.057)	(0.020)	(0.019)
time2010	−0.593***	−0.914***	−0.862***
	(0.057)	(0.023)	(0.022)
time2011	−0.729***	−0.996v	−0.966***
	(0.058)	(0.022)	(0.021)
time2012	−0.724***	−1.023***	−0.983***
	(0.058)	(0.022)	(0.021)
time2013	−0.781***	−1.110***	−1.063***
	(0.058)	(0.024)	(0.022)
time2014	−0.857***	−1.142***	−1.115***
	(0.058)	(0.024)	(0.023)
time2015	−0.871***	−1.185***	−1.151***
	(0.058)	(0.024)	(0.023)
time2016	−0.902***	−1.264***	−1.222***
	(0.059)	(0.026)	(0.025)
time2017	−0.904***	−1.297***	−1.252***
	(0.059)	(0.027)	(0.026)
Constant	−53.402***	–	70.194***
	(12.654)	–	(12.754)
Observations	16,596	16,596	16,596
R^2	0.287	0.548	0.533
Adjusted R^2	0.286	0.520	0.532

Notes:
***Significant at the 1 percent level.
**Significant at the 5 percent level.
*Significant at the 10 percent level.

Table A10
Test to evaluate the most relevant spatial model.

	Estimate	Std.error	t-value	Pr(>|t|)
CO_2				
Lambda	−0.4417129	0.03344362	−13.20769	7.922096e-40
rho	0.7678899	0.01037133	74.03966	0.000000e+00
$PM_{2.5}$				
Lambda	−0.8483532	0.035445381	−23.93410	1.353058e-126
rho	0.7987469	0.008551844	93.40055	0.000000e+00
O_3				
Lambda	−0.5405122	0.035386664	−15.27446	1.131591e-52
rho	0.8796115	0.006179993	142.33214	0.000000e+00
AA				
Lambda	0.6504746	0.03189511	20.394180	1.883472e-92
rho	−0.5798640	0.08652545	−6.701658	2.060678e-11
SO_2				
Lambda	0.457346	0.034096	13.414	0.000000e+00
rho	−0.338973	0.060169	−5.6337	1.764e-08

Table A11
Estimation results for the EKC shape coefficients values (log GDP, $\log GDP^2$, $\log GDP^3$) and the spatial error parameter rho for each indicator varying the number of neighbours in the spatial weight matrix.

Indicator	Coefficients	K = 1	K = 5	K = 25	K = 50
CO_2	β_1	1.400	1.427	1.515	1.501
	β_2	−0.056	−0.058	−0.060	−0.063
	β_3	–	–	–	–
	Rho	0.070	0.205	0.507	0.638
O_3	β_1	−43.500	−21.600	−12.7612	−10.858
	β_2	4.030	2.044	1.1920	1.001
	β_3	−0.1245	−0.063	−0.037	−0.0313
	Rho	0.3000	0.561	0.797	0.870
$PM_{2.5}$	β_1	1.732	2.312	2.543	2.416
	β_2	−0.163	−0.220	−0.245	−0.235
	β_3	0.005	0.006	0.008	0.007
	Rho	0.168	0.427	0.700	0.774
AA	β_1	−3.806	−3.398	−2.934	−2.733
	β_2	0.395	0.353	0.306	0.286
	β_3	−0.013	−0.012	−0.010	−0.009
	Rho	0.059	0.254	0.536	0.685
SO_2	β_1	−9.807	−9.890	−9.859	−9.678
	β_2	0.876	0.886	0.890	0.871
	β_3	−0.0247	−0.025	−0.025	−0.025
	Rho	0.0334	0.155	0.350	0.454

(2022), who investigated the EKC in 134 countries and found that urbanisation diminishes the benefits of economic growth on emissions reduction. In response to this trend, cities with a higher emission growth are more likely to join TCNs.

Regarding ozone, both member and non-member cities display negative marginal effects consistent with full sample estimates. Considering land use, both groups return evidence consistent with the EKC hypothesis, but member cities are characterised by a lower turning point (4,400 USD vs 6,000 USD and 40,100 USD vs 120,500 USD). The $PM_{2.5}$ results deserve special attention. While member cities display an air pollution reduction trajectory similar to that displayed by the full sample, non-member cities' trajectory is not even comparable. The non-member cities' marginal effect is always positive, without a turning point.

Fig. 6 depicts the spatial distribution of cities depending on their current decoupling stage. For CO_2 emissions, most of the cities in the

Table A12
Full estimation results for CO_2 emissions, O_3 and $PM_{2.5}$, concentrations, and artificial Land Use. Standard Error in parenthesis. The specification for CO_2 does not include $\log GDP^3$ due to non significance. The model for $PM_{2.5}$ is fitted with GMM estimation.

	CO_2	O_3	$PM_{2.5}$	Land Use
log_G	1.631***	−9.621**	2.853***	−3.116***
	(1.842)	(3.516)	(0.613)	(0.534)
log_G_2	−0.058***	0.896**	−0.272***	0.326***
	(0.008)	(0.326)	(0.060)	(0.052)
log_G_3	–	−0.028**	0.008***	−0.011***
		(0.010)	(0.001)	(0.001)
log_D	−0.310***	−0.003	0.058*	0.131***
	(0.005)	(0.007)	(0.012)	(0.013)
log_Temp	5.321***	31.725***	−9.978***	4.010***
	(0.790)	(0.960)	(0.744)	(0.827)
City Network	0.050***	−0.024	0.027***	0.016
	(0.013)	(0.015)	(0.003)	(0.003)
time 2001	−0.004	–	−0.018	–
	(0.027)		(0.010)	
time 2002	−0.017	–	0.083***	–
	(0.027)		(0.010)	
time 2003	0.028	–	0.112***	–
	(0.027)		(0.010)	
time 2004	0.042	–	−0.060***	–
	(0.028)		(0.010)	
time 2005	0.071*	–	0.033**	–
	(0.028)		(0.010)	
time 2006	0.021	–	0.068***	0.060***
	(0.028)		(0.010)	(0.005)
time 2007	−0.024	−0.800***	−0.112***	–
	(0.028)	(0.030)	(0.010)	
time 2008	−0.084**	−0.317***	−0.171***	–
	(0.028)	(0.030)	(0.011)	
time 2009	−0.151***	−0.408***	−0.167***	–
	(0.028)	(0.030)	(0.010)	
time 2010	−0.192***	−0.355***	−0.139***	–
	(0.028)	(0.031)	(0.011)	
time 2011	−0.278***	−0355***	−0.088***	–
	(0.028)	(0.030)	(0.011)	
time 2012	−0.289***	−0.424***	−0.161***	0.090***
	(0.028)	(0.031)	(0.011)	(0.006)
time 2013	−0.312***	−0.393***	−0.200***	–
	(0.029)	(0.031)	(0.011)	
time 2014	−0.408***	−0.685***	−0.037***	–
	(0.029)	(0.031)	(0.011)	
time 2015	−0.410***	−0.758***	−0.092***	–
	(0.029)	(0.031)	(0.011)	
time 2016	−0.447***	−0.600***	−0.085***	
	(0.029)	(0.031)	(0.012)	
time 2017	−0.457***	−0.841***	−0.011	–
	(0.029)	(0–031)	(0.012)	
time 2018	−0.506**	−0.148***	0.039**	0.071***
	(0.029)	(0.031)	(0.012)	(0.008)
Rho (spatial error parameter)	0.495***	0.532***	0.523***	0.408***
	(0.011)	(0.013)	(0.011)	(0.028)
Observations	17,518	11,986	15,674	3688
R^2	0.329	0.532	0.9391	0.9944

decoupling stage are non-members[22] and concentrated in the United Kingdom and Germany. For $PM_{2.5}$ concentrations, there is no spatial pattern, but the gap between members and non-members is clear: member cities are all in the decoupling stage, while the totality of non-members is still in the first stage. Finally, no spatial pattern can be found in the distribution of decoupling cities for AA.

5. Discussion

To make sense of these results, the average trends in environmental degradation in Fig. 2 can be compared with the distribution of decoupling cities in Fig. 6. European cities are largely on track in their decoupling efforts for $PM_{2.5}$ and O_3 concentrations, as most of them (respectively, 477 and 922 out of 922) have an average per capita income that is greater than that required to decouple environmental degradation from development. This conclusion is in line with the decreasing trends in environmental degradation at the aggregate European level (see Fig. 2). In particular, the findings confirm that network participation is associated with improved urban air quality by facilitating the decoupling of economic development from pollution. This is crucial for European cities, where the share of the population exposed to annual averages of $PM_{2.5}$ and O_3 concentration levels above 2021 WHO thresholds was about 96%–100% and 93%–98%, respectively (EEA, 2022).

European cities are also on track with reduction of soil sealing. However, there is strong evidence that sprawl is the predominant urban spatial expansion model in Europe, with 654 sample cities lagging behind the second turning point. Evidence suggests that TCNs appear to contribute in this context, promoting several initiatives to reduce artificial areas in urban centres. For example, the C40 Land Use Planning Network provides a platform for cities to accelerate the development and implementation of sustainable and inclusive land-use policies, such as 15-minutes city policies and the preservation of green spaces. The European Covenant of Mayors considers land-use planning as one of the most vulnerable sectors on the adaptation side and prescribes a minimum share of green surface area among the policy instruments in cases of urban expansion (JRC, 2016). ICLEI-led INTERACT-Bio, although currently focused on the Global South, provides nature-based solutions to expanding urban communities and is designed to improve the management of nature within cities.

This study's results point towards a novel city-based interpretation of the drivers of the EKC curvature: multi-lateral interaction. In fact, it found that cities achieve a balance between economic development and sustainability by participating in climate protection networks, benefitting from informal regulation and knowledge spill-overs from peers. This hypothesis is line with Hawkins et al. (2016), who used survey data of US state governments to conclude that network participation is a strong predictor of local policy decisions on environmental issues. One possible channel harnessing these dynamics is the so-called "networked experimentation" (Smeds and Acuto, 2018). For local governments, networking facilitates knowledge-sharing and learning, potentially giving policymakers ideas and confidence to conduct experiments. Another channel is enabled by the involvement of interest groups in city politics. In fact, multi-lateral networking can cause the birth of local environmental advocacy groups, whose inclusion in policymaking may spur a high number of programs aimed at achieving sustainability (Berry and Portney, 2013).

To further corroborate this study's hypothesis, another type of strategic interaction between local governments that may help flatten the pollution curve was examined: Chinese intergovernmental competition (IGC). In 2007, the Chinese central government enforced an environmental target responsibility system (TRS) and introduced environmental indicators to an official ranking tournament. Following this scheme, local governments are ranked according to their environmental performance and laggards are economically sanctioned. Zhang and Yang (2022) found that local officials tailor their enforcement of top-down environmental policies to balance and align their environmental performance with that of their peer competitors. The authors highlighted the role of peer pressure between Chinese local authorities in pushing down the EKC for 84 cities, reflecting the same effect of TCNs on the EKC in Europe.

The most straightforward policy implication ensuing from these results would be that non-member cities should consider joining sustainability-related TCNs, in order to benefit from the positive externalities such as knowledge spillovers. Moreover, member cities that are not yet in the decoupling stage of development could compare their degree of involvement and the selected actions and projects against the

[22] There is only one member city in the decoupling stage for CO_2 emissions: Southampton, UK.

ones of decoupled cities.

6. Concluding remarks

Urban growth has traditionally been the flywheel of economic development, and Europe is no exception. Too often and too greatly, this has come at the price of environmental degradation and natural resources' depletion. The extent to which modern cities can reverse this course and enter the path of sustainable development is a crucial issue in light of climate change and biodiversity losses. City networks can guide towards this path by promoting best-practice sharing and delivering science-based policy guidance.

This paper explores the issue in depth. It leverages satellite data availability to build a set of environmental indicators able to represent environmental degradation over time and at a high spatial resolution. This enables the urban scale to be viewed directly in the empirical investigation, considering the multiple faces of environmental degradation stemming from carbon emissions to pollutant concentration in the air and natural resources depletion, soil in particular. By doing so, it becomes possible to view cities as units in an environmental decoupling analysis, thus contributing to a literature that has primarily focused on country-level analyses.

The study found evidence overall consistent with the EKC hypothesis, which predicts environmental degradation to increase during the developing stages and fall once wealthier conditions are achieved. Although this evidence is largely heterogeneous across the environmental degradation indicators considered, the general message is that European cities are on track to achieve sustainable development. The estimated income level at which environmental degradation starts to fall is relatively small, with many cities having already passed this threshold and even more being close to doing so. Carbon and sulphur dioxide emissions are exceptions. In the first case, evidence suggests that European cities have not been able to decouple their economic growth from carbon emissions, notwithstanding the general emission reduction trend in Europe. In the second case, there was less robust evidence because sulphur dioxide concentration has been steadily declining in European cities and is now well below the safe level.

The second piece of evidence concerns the role of TCNs. Unfortunately, the empirical basis in this paper does not allow a conclusion based on causal inference, as it lacks a pure counter-factual approach. However, the paper has the merit of being the first to look at the issue, even if it does so by considering only potential correlation. The exciting evidence that emerges is that there is a connection between TCNs and the shape of the EKC. Participating cities are better on track to sustainability compared to their non-participating counterparts. A larger share of participating cities either have already crossed the critical threshold or are close to doing so. Of course, it must be acknowledged that participating cities are likely to be larger and more developed and, hence, more polluted and this may cause them to fall in the advanced stages of the EKC. This would cause a participation bias that is only possible to address with a serious counter-factual approach that is, as said before, outside the scope of this work.

The findings of this study suggest that city governments should engage with TCNs and adopt common solutions for transitioning to a low-carbon economy. Multilateral interaction through city diplomacy and participation in networks can provide many benefits. For example, they facilitate informal regulation and promote knowledge sharing between cities. Additionally, they can bolster the efforts of local environmental advocacy groups, which can help drive sustainable policy agendas. However, there are some caveats to this recommendation. According to Haupt and Coppola (2019), some studies suggest that the economic costs and technical expertise required to join these networks may outweigh the benefits. Therefore, city governments should carefully consider the trade-offs involved in joining a particular network. For instance, Cortes Berrueta and van der Heijden (2021) analyse these trade-offs and identify three key underlying factors: the clarity of the promised benefits, the combination of requirements and commitments, and the explicitness of the network's targets.

In conclusion, more research on environmental decoupling at the local level is needed. The latter can help local governments make informed policy decisions, such as the effectiveness involved in joining climate protection networks.

CRediT authorship contribution statement

Massimiliano Carlo Pietro Rizzati: Conceptualization, Data curation, Software, Writing – original draft, Writing – review & editing. **Nicolò Florenzio:** Conceptualization, Data curation, Software, Writing – original draft, Writing – review & editing. **Gianni Guastella:** Conceptualization, Methodology, Writing – original draft, Writing – review & editing. **Stefano Pareglio:** Conceptualization, Supervision, Project administration, Resources, Writing – review & editing.

Declaration of Competing Interest

The authors declare that they have no known competing financial interests or personal relationships that could have appeared to influence the work reported in this paper.

Data availability

Data will be made available on request.

Acknowledgements

We gratefully acknowledge the comments and suggestions from the participants in the tenth Italian Association of Environmental and Resource Economists (IAERE) Annual Conference (Cagliari, April 21-23, 2022). Errors remain our own. M. Rizzati, N. Florenzio, G. Guastella and S. Pareglio did not receive any specific grant from funding agencies in the public, commercial or not-for-profit sectors.

Appendix

Fig. A1.

Table A1. Table A2. Table A3. Table A4. Table A5. Table A6. Table A7. Table A8. Table A9. Table A10. Table A11. .

References

Acaravci, A., Ozturk, I., 2010. On the relationship between energy consumption, CO_2 emissions and economic growth in Europe. Energy 35 (12), 5412–5420.

Acuto, M., Leffel, B., 2021. Understanding the global ecosystem of city networks. Urban Stud. 58 (9), 1758–1774.

Aldy, J.E., 2005. An environmental Kuznets Curve analysis of U.S. State-level carbon dioxide emissions. J. Environ. Dev. 14 (1), 48–72.

Altıntaş, H., Kassouri, Y., 2020. Is the environmental Kuznets Curve in Europe related to the per-capita ecological footprint or CO2 emissions? Ecol. Ind. 113, 106187.

Baltagi, B.H., Song, S.H., Jung, B., Koh, W., 2007. Testing panel data regression models with spatial and serial error correlation. J. Econ. 140, 5–51.

Baltagi, B.H. (2021*). Econometric analysis of panel data* (vol. 4, sixth edition). John Wiley & Sons: Chichester.

Beenstock, M., Felsenstein, D., 2019. The econometric analysis of non-stationary spatial panel data. Springer International Publishing.

Berry, J.M., Portney, K.E., 2013. Sustainability and interest group participation in city politics. Sustainability 5 (5), 2077–2097.

Bimonte, S., Stabile, A., 2017. Land consumption and income in Italy: a case of inverted EKC. Ecol. Econ. 131, 36–43.

Bivand, R., Altman, M., Anselin, L., Assunção, R., Berke, O., Bernat, A., Blanchet, G. (2015). Package 'spdep'. *The Comprehensive R Archive Network*.

Bivand, R., Millo, G., Piras, G., 2021. A review of software for spatial econometrics in R. Mathematics 9 (11), 1276.

Bölük, G., Mert, M., 2014. Fossil & renewable energy consumption, GHGs (greenhouse gases) and economic growth: Evidence from a panel of EU (European Union) countries. Energy 74, 439–446. https://doi.org/10.1016/j.energy.2014.07.008.

Boubellouta, B., Kusch-Brandt, S., 2020. Testing the environmental Kuznets Curve hypothesis for E-waste in the EU28+ 2 countries. J. Clean. Prod. 277, 123371.

Cho, C.H., Chu, Y.P., Yang, H.Y., 2014. An environment Kuznets curve for GHG emissions: a panel cointegration analysis. Energy Sources Part B 9 (2), 120–129.
Cole, M.A., 2003. Development, trade, and the environment: how robust is the Environmental Kuznets Curve? Environ. Dev. Econ. 8 (4), 557–580.
Cortes Berrueta, S., van der Heijden, J., 2021. Trading off benefits and requirements: how do city networks attract cities to their voluntary environmental programmes? Environ. Policy Gov. 31 (5), 451–462.
Crippa, M., Guizzardi, D., Butler, T., Keating, T., Kaminski, J., Kuenen, J., Kurokawa, J., Satoru, C., Pouliot, G., Racine, J., Moran, M., Klimont, Z., Wu, R., Manseau, P., Barron, H., Smith, S., Muntean, M., Solazzo, E., Banja, M., Schaaf, E., Pagani, F., Monforti, F., Pisoni, E. (in preparation). HTAPv3 emission mosaic: a global effort to tackle air quality issues. European Commission, Joint Research Centre (EC-JRC)/ Netherlands Environmental Assessment Agency (PBL). Emissions Database for Global Atmospheric Research (EDGAR), release EDGAR v6.1_AP (1970–2018) Link: https://edgar.jrc.ec.europa.eu/dataset_htap_v3.
Croissant, Y., Millo, G., 2008. Panel data econometrics in R: The plm package. J. Stat. Softw. 27 (2).
Cuaresma, J.C., Danylo, O., Fritz, S., McCallum, I., Obersteiner, M., See, L., Walsh, B., 2017. Economic development and forest cover: evidence from satellite data. Sci. Rep. 7 (1), 1–8.
Dent, C.M., Bale, C., Wadud, Z., Voss, H., 2016. Cities, energy and climate change mitigation: an introduction. Cities 54, 1–3.
Ding, Y., Zhang, M., Chen, S., Wang, W., Nie, R., 2019. The environmental Kuznets curve for PM2. 5 pollution in Beijing-Tianjin-Hebei region of China: a spatial panel data approach. J. Clean. Prod. 220, 984–994.
European Environmental Agency. (2018). European air quality maps for 20–8 - PM10, PM2.5, Ozone, NO_2 and NOx Spatial estimates and their uncertainties (Eionet Repo–t - ETC/ATNI 2020/10).
European Environmental Agency. (2021). Emissions of the main air pollutants in Europe. Link: https://www.eea.europa.eu/ims/emissions-of-the-main-air.
European Environmental Agency. (2021). Emissions of ozone precursors. Link: https://www.eea.europa.eu/data-and-maps/indicators/emissions-of-ozone-precursors-version-2/assessment-4.
European Environmental Agency. (2021). EEA greenhouse gases - data viewer. Link: https://www.eea.europa.eu/data-and-maps/data/data-viewers/greenhouse-gases-viewer.
European Environmental Agency. (2021). Land cover country fact sheets 2000-2018. Link: https://www.eea.europa.eu/themes/landuse/land-cover-country-fact-sheets.
European Environmental Agency. (2022). Exceedance of air quality standards in Europe. Link: https://www.eea.europa.eu/ims/exceedance-of-air-quality-standards.
European Environmental Agency. (2022). Air quality report 2022. Link: https://www.eea.europa.eu/publications/air-quality-in-europe-2022/sources-and-emissions-of-air.
European Union. Copernicus Land Monitoring Service 2000, 2006, 2012, 2018 European Environment Agency (EEA).
European Environment Agency, 2019. Land and soil in Europe — Ever-sprawling urban concrete?. https://www.eea.europa.eu/signals/signals-2019-content-list/articles/land-and-soil-in-europe.
Fang, C., Liu, H., Wang, S., 2021. The coupling curve between urbanisation and the eco-environment: China's urban agglomeration as a case study. Ecol. Ind. 130, 108107.
Floater, G., Rode, P., Robert, A., Kennedy, C., Hoornweg, D., Slavcheva, R., & Godfrey, N. (2014). Cities and the new climate economy: the transformative role of global urban growth. LSE eprints, NCE Cities – Paper 01.
Fragkias, M., Lobo, J., Strumsky, D., Seto, K.C., Convertino, M., 2013. Does size matter? Scaling of CO_2 emissions and US urban areas. PLoS One 8 (6), e64727.
Fujii, H., Iwata, K., Chapman, A., Kagawa, S., Managi, S., 2018. An analysis of urban environmental Kuznets curve of CO_2 emissions: empirical analysis of 276 global metropolitan areas. Appl. Energy 228, 1561–1568.
Galeotti, M., Lanza, A., 1999. Richer and cleaner? A study on carbon dioxide emissions in developing countries. Energy Policy 27 (10), 565–573.
Galeotti, M., Lanza, A., Pauli, F., 2006. Reassessing the environmental Kuznets curve for CO_2 emissions: a robustness exercise. Ecol. Econ. 57 (1), 152–163.
Galeotti, M., Manera, M., Lanza, A., 2009. On the robustness of robustness checks of the environmental Kuznets curve hypothesis. Environ. Resour. Econ. 42 (4), 551–574.
Gately, C.K., Hutyra, L.R., Wing, I.S., 2015. Cities, traffic, and CO2: A multidecadal assessment of trends, drivers, and scaling relationships. Proc. Natl. Acad. Sci. 112 (16), 4999–5004.
Germani, A.R., Ker, A.P., Castaldo, A., 2020. On the existence and shape of an environmental crime Kuznets Curve: a case study of Italian provinces. Ecol. Ind. 108.
Grossman, G.M., Krueger, A.B., 1995. Economic growth and the environment. Q. J. Econ. 110 (2), 353–377.
Guastella, G., Oueslati, W., Pareglio, S., 2019. Patterns of urban spatial expansion in European cities. Sustainability 11 (8), 2247.
Guastella, G.i., Pareglio, S., Sckokai, P., 2017. A spatial econometric analysis of land use efficiency in large and small municipalities. Land Use Policy 63, 288–297.
Gurney, K.R., Liang, J., O'Keeffe, D., Patarasuk, R., Hutchins, M., Huang, J., Song, Y., 2019. Comparison of global downscaled versus bottom-up fossil fuel CO_2 emissions at the urban scale in four US urban areas. J. Geophys. Res. Atmos. 124 (5), 2823–2840.
Hao, Y., Liu, Y., Weng, J.-H., Gao, Y., 2016. Does the Environmental Kuznets Curve for coal consumption in China exist? New evidence from spatial econometric analysis. Energy 114, 1214–1223.
Harris, R.D., Tzavalis, E., 1999. Inference for unit roots in dynamic panels where the time dimension is fixed. J. Econ. 91 (2), 201–226.
Haupt, W., Coppola, A., 2019. Climate governance in transnational municipal networks: advancing a potential agenda for analysis and typology. Int. J. Urban Sustain. Dev. 11 (2), 123–140.
Hawkins, C.V., Kwon, S.W., Bae, J., 2016. Environmental sustainability: a multi-level governance perspective. Int. J. Public Adm. 39 (11), 803–811.
Hsu, A., Tan, J., Ng, Y.M., Toh, W., Vanda, R., Goyal, N., 2020. Performance determinants show European cities are delivering on climate mitigation. Nat. Clim. Chang. 10 (11), 1015–1022.
Im, K.S., Pesaran, M.H., Shin, Y., 2003. Testing for unit roots in heterogeneous panels. J. Econ. 115 (1), 53–74.
Jacobs, J., 1969. The Economy of Cities. Random House, New York, United States.
Joint Research Centre of the European Commission. (2016). The Covenant of Mayors for Climate and Energy Reporting Guidelines. Link: https://www.covenantofmayors.eu/IMG/pdf/Covenant_ReportingGuidelines.pdf.
Kang, Y.Q., Zhao, T., Yang, Y.Y., 2016. Environmental Kuznets curve for CO_2 emissions in China: a spatial panel data approach. Ecol. Ind. 63, 231–239.
Kapos, V., 2000. UNEP-WCMC Web site: mountains and mountain forests. Mt. Res. Dev. 20 (4), 378.
Kasman, A., Duman, Y.S., 2015. CO2 emissions, economic growth, energy consumption, trade and urbanization in new EU member and candidate countries: A panel data analysis. Economic Modelling 44, 97–103. https://doi.org/10.1016/j.econmod.2014.10.022.
Kaufmann, R.K., Davidsdottir, B., Garnham, S., Pauly, P., 1998. The determinants of atmospheric SO_2 concentrations: reconsidering the environmental Kuznets curve. Ecol. Econ. 25 (2), 209–220.
Kona, A., Bertoldi, P., Monforti-Ferrario, F., Rivas, S., Dallemand, J.F., 2018. Covenant of mayors signatories leading the way towards 1.5 degree global warming pathway. Sustain. Cities Soc. 41, 568–575.
Kona, A., Monforti-Ferrario, F., Bertoldi, P., Baldi, M.G., Kakoulaki, G., Vetters, N., Thiel, C., Melica, G., Lo Vullo, E., Sgobbi, A., Ahlgren, C., Posnic, B., 2021. Global Covenant of Mayors, a dataset of greenhouse gas emissions for 6200 cities in Europe and the Southern Mediterranean countries. Earth Syst. Sci. Data 13 (7), 3551–3564.
Krugman, P., 1991. Increasing returns and economic geography. J. Polit. Econ. 99 (3), 483–499.
Labaeye, A., Sauer, T. (2013). City networks and the socio-ecological transition. A European inventory. WWW for Europe Working Paper No. 27. WIFO Studies.
Lauvaux, T., Gurney, K.R., Miles, N.L., Davis, K.J., Richardson, S.J., Deng, A., Nathan, B. J., Oda, T., Wang, J.A., Hutyra, L., Turnbull, J., 2020. Policy-relevant assessment of urban CO_2 emissions. Environ. Sci. Tech. 54 (16), 10237–10245.
LeSage, J.P., Pace, R.K., 2014. The biggest myth in spatial econometrics. Econometrics 2 (4), 217–249.
Liu, J., Guo, Q., 2015. A spatial panel statistical analysis on cultivated land conversion and Chinese economic growth. Ecol. Ind. 51, 20–24.
Maddison, D., 2006. Environmental Kuznets curves: a spatial econometric approach. J. Environ. Econ. Manag. 51 (2), 218–230.
Makido, Y., Dhakal, S., Yamagata, Y., 2012. Relationship between urban form and CO_2 emissions: evidence from fifty Japanese cities. Urban Clim. 2, 55–67.
Maranzano, P., Cerdeira Bento, J.P., Manera, M., 2022. The role of education and income inequality on environmental quality: a panel data analysis of the EKC hypothesis on OECD countries. Sustainability 14 (3), 1622.
Millo, G., Piras, G., 2012. splm: spatial panel data models in R. J. Stat. Softw. 47, 1–38.
Muñoz Sabater, J. (2019). ERA5-Land hourly data from 1981 to present, Copernicus Climate Change Service (C3S) Climate Data Store (CDS).
Moran, D., Pichler, P.-P., Zheng, H., Muri, H., Klenner, J., Kramel, D., Többen, J., Weisz, H., Wiedmann, T., Wyckmans, A., Strømman, A.H., Gurney, K., n.d.. R., 2022. Estimating CO2 emissions for 108 000 European cities. Earth Syst. Sci. Data 14, 845–864. https://doi.org/10.5194/essd-14-845-2022.
Nguyen, T.M.P., Davidson, K., Coenen, L., 2020. Understanding how city networks are leveraging climate action: experimentation through C40. Urban Transformations 2 (1), 1–23.
Oda, T., Bun, R., Kinakh, V., Topylko, P., Halushchak, M., Marland, G., Lauvaux, T., Jonas, M., Maksyutov, S., Nahorski, Z., Lesiv, M., Danylo, O., Horabik-Pyzel, J., 2019. Errors and uncertainties in a gridded carbon dioxide emissions inventory. Mitig. Adapt. Strat. Glob. Chang. 24 (6), 1007–1050.
OECD (2018). OECD regions and cities at a glance.
Overman, H.G., Puga, D., 2010. Labor Pooling as a Source of Agglomeration: An Empirical Investigation. University of Chicago Press, Chicago, pp. 133–150.
Pan, G., Xu, Y., Ma, J., 2021. The potential of CO_2 satellite monitoring for climate governance: a review. J. Environ. Manage. 277, 111423.
Pesaran, M.H., 2007. A simple panel unit root test in the presence of cross-section dependence. J. Appl. Economet. 22 (2), 265–312.
Pontarollo, N., Mendieta Muñoz, R., 2020. Land consumption and income in Ecuador: a case of an inverted environmental Kuznets curve. Ecol. Ind. 108, 105699.
Pontarollo, N., Serpieri, C., 2020. Testing the Environmental Kuznets Curve hypothesis on land use: the case of Romania. Land Use Policy 97, 104695.
Rafaj, P., Amann, M., Siri, J.G., 2014. Factorisation of air pollutant emissions: projections versus observed trends in Europe. Sci. Total Environ. 494, 272–282.
Rashidi, K., Patt, A., 2018. Subsistence over symbolism: the role of transnational municipal networks on cities' climate policy innovation and adoption. Mitig. Adapt. Strat. Glob. Chang. 23 (4), 507–523.
Ribeiro, H.V., Rybski, D., Kropp, J.P., 2019. Effects of changing population or density on urban carbon dioxide emissions. Nat. Commun. 10 (1), 1–9.
Rupasingha, A., Goetz, S.J., Debertin, D.L., Pagoulatos, A., 2004. The environmental Kuznets curve for US counties: a spatial econometric analysis with extensions. Papers Reg. Sci. 83 (2), 407–424.

Sarkodie, S.A., Strezov, V., 2019. A review on environmental Kuznets curve hypothesis using bibliometric and meta-analysis. Sci. Total Environ. 649, 128–145.
Selden, T.M., Song, D., 1994. Environmental quality and development: is there a Kuznets curve for air pollution emissions? J. Environ. Econ. Manag. 27 (2), 147–162.
Shafiei, S., Salim, R.A., 2014. Non-renewable and renewable energy consumption and CO_2 emissions in OECD countries: a comparative analysis. Energy Policy 66, 547–556.
Shahbaz, M., Sinha, A., 2019. Environmental Kuznets curve for CO_2 emissions: a literature survey. J. Econ. Stud. 46 (1), 106–168.
Sinha, A., Bhattacharya, J., 2017. Estimation of environmental Kuznets curve for SO_2 emission: a case of Indian cities. Ecol. Ind. 72, 881–894.
Smeds, E., Acuto, M., 2018. Networking cities after Paris: weighing the ambition of urban climate change experimentation. Global Pol. 9 (4), 549–559.
Stern, D.I., Common, M.S., Barbier, E.B., 1996. Economic growth and environmental degradation: the environmental Kuznets curve and sustainable development. World Dev. 24 (7), 1151–1160.
Tiseo, I. (2022). Breakdown of CO2 Emissions in the EU-27, by sector. Statista. Link: https://www.statista.com/statistics/1240108/road-transportation-greenhouse-gas-emissions-eu/.
UN Environment Programme (n.d.).Cities and Climate Change. Link: https://www.unep.org/explore-topics/resource-efficiency/what-we-do/cities/cities-and-climate-change.
UN-Habitat (2020). World Cities Report 2020. Envisaging the Future of Cities. Link: https://unhabitat.org/sites/default/files/2022/06/wcr_2022.pdf.
van Donkelaar, A., Martin, R. V., Brauer, M., Hsu, N.C., Kahn, R. A., Levy, R. C., Lyapustin, A., Sayer, A. M., Winker, D. M. (2018). *Global Annual PM2.5 Grids from MODIS, MISR and SeaWiFS Aerosol Optical Depth (AOD) with GWR, 1998-2016*. Socioeconomic Data and Applications Center (SEDAC), NASA: Palisades, New York, United States. Link: https://doi.org/10.7927/H4ZK5DQS.
Wang, Y., Kang, L., Wu, X., Xiao, Y., 2013. Estimating the environmental Kuznets curve for ecological footprint at the global level: a spatial econometric approach. Ecol. Ind. 34, 15–21.
Wang, H., Lu, X., Deng, Y., Sun, Y., Nielsen, C.P., Liu, Y., Zhu, G., Bu, M., Bi, J., McElroy, M.B., 2019. China's CO_2 peak before 2030 implied from characteristics and growth of cities. Nat. Sustainability 2 (8), 748–754.
Wang, Q., Wang, X., Li, R., 2022. Does urbanization redefine the environmental Kuznets curve? An empirical analysis of 134 Countries. Sustainable Cities Soc. 76, 103382.
Wang, Z., Ye, X., 2017. Re-examining environmental Kuznets curve for China's city-level carbon dioxide (CO_2) emissions. Spatial Statistics 21, 377–389.
World Bank. (2022). Urban Development. Link: https://www.worldbank.org/en/topic/urbandevelopment/overview.
World Economic Forum. (2022). BiodiverCities by 2030: Transforming Cities Relationship with Nature. Link: https://www3.weforum.org/docs/WEF_BiodiverCities_by_2030_2022.pdf.
Wu, D., Lin, J.C., Oda, T., Kort, E.A., 2020. Space-based quantification of per capita CO_2 emissions from cities. Environ. Res. Lett. 15 (3), 035004.
Xu, C., Yiwen, Z., Cheng, B., Li, L., Zhang, M., 2020. Study on environmental Kuznets curve for noise pollution: a case of 111 Chinese cities. Sustain. Cities Soc. 63, 102493.
Yang, E.G., Kort, E.A., Wu, D., Lin, J.C., Oda, T., Ye, X., Lauvaux, T., 2020. Using space-based observations and Lagrangian modeling to evaluate urban carbon dioxide emissions in the Middle East. J. Geophys. Res. Atmos. 125 (7).
Zhang, Z., Yang, M., 2022. Reexamining the Environmental Kuznets Curve in Chinese cities: does intergovernmental competition matter? Int. J. Environ. Res. Public Health 19, 14989.
Zheng, S., Kahn, M.E., 2017. A new era of pollution progress in urban China? J. Econ. Perspect. 31 (1), 71–92.
Zoundi, Z., 2017. CO_2 emissions, renewable energy and the Environmental Kuznets Curve, a panel cointegration approach. Renew. Sustain. Energy Rev. 72, 1067–1075.

Further reading

Corfee-Morlot, J., Kamal-Chaoui, L., Donovan, M. G., Cochran, I., Robert, A., Teasdale, P. J. (2009). Cities, climate change and multilevel governance. OECD Environmental Working Papers N° 14, 2009, OECD Publishing.
Elhorst, J. (2009). Spatial panel data models in Fischer, M.M., & Getis, A. (eds.) *Handbook of Applied Spatial Analysis* Springer: New York.
European Environmental Agency. (2017). Sector share of sulphure oxides emissions – 2009 (EEA member countries). Link: https://www.eea.europa.eu/data-and-maps/figures/sector-share-of-sulphur-dioxide-emissions-eea-member-countries-2.
Eurostat. (2016), Urban Europe — statistics on cities, towns and suburbs. Link: https://ec.europa.urostattat/web/products-statistical-books/-/KS-01-16-691.
Stern, D.I., 2004. The rise and fall of the environmental Kuznets curve. World Dev. 32 (8), 1419–1439.
Sinha, A., Shahbaz, M., Balsalobre, D. (2018). N-shaped environmental Kuznets curve: a note on validation and falsification. *MPRA Paper* No. 99313.
UN-Habitat (2011). Global Report on Human Settlements: Cities and Climate Change. Link: https://unhabitat.org/global-report-on-human-settlements-2011-cities-and-climate-change.
UN-Habitat (2016). World City Report 2016. Urbanisation and Development: Emerging Futures. Link: https://unhabitat.org/sites/default/files/download-manager-files/WCR-2016-WEB.pdf.